antitumour activity of NK105 was significantly more potent than that of free PTX, probably because of enhanced tumour exposure through the EPR effect (Hamaguchi et al, 2005).

We conducted a phase I clinical trial using NK105 in patients with advanced solid tumours. The objectives of this trial were to determine the maximum tolerated dose (MTD), the phase II recommended dose (RD), and the pharmacokinetics of NK105.

PATIENTS AND METHODS

The protocol and all materials were approved by the Institutional Review Board of the National Cancer Center, Tokyo. This study was conducted in compliance with the Good Clinical Practice Guidelines of the International Conference on Harmonization and the Declaration of Helsinki Principles. Written informed consent was obtained from all the patients.

Therapeutic agent

NK105 was supplied by Nippon Kayaku Co. Ltd. (Tokyo, Japan) in 20-ml glass vials containing a dose equivalent to 30 mg of PTX. When reconstituted in 10 ml of 5% glucose solution and diluted with a total volume of 250 ml of 5% glucose, the reconstituted solution was stable for 24 h at room temperature. In our preclinical study, DLS and HPLC analysis showed that less than 2% of PTX incorporated in the micelles was released for 24 h at room temperature (data not shown).

Figure 1 shows the schematic structure of NK105, a PTX-entrapped polymeric micelle formulation. The NK105 polymers were constructed using polyethylene glycol (PEG) as the hydrophilic component and modified polyaspartate as the hydrophobic component. PEG is believed to form the outer shell of the micelle, producing a 'stealth' effect that enables NK105 to avoid being captured by the reticuloendothelial system.

The modified polyaspartate chain is hydrophobic and is believed to form the hydrophobic inner core of the micelles in aqueous media. The hydrophobic inner core enables NK105 to entrap a sufficient amount of PTX. NK105 has a diameter of about 90 nm (Hamaguchi et al, 2005).

Patients

Patients with solid tumours refractory to conventional chemotherapy and for whom no effective therapy was available were eligible for enrolment in this study, provided that the following criteria were met: a histologically confirmed malignant tumour; a performance status of $\leqslant 2$; an age of $\geqslant 20$ and < 75 years; a normal haematological profile (neutrophil count $\geqslant 2000$ mm^{-3}, platelet count $\geqslant 100\,000$ mm^{-3}, hemoglobin $\geqslant 9$ g dl^{-1}); normal hepatic function (total bilirubin level $\leqslant 1.5$ mg dl^{-1}, AST and ALT $\leqslant 2.5$
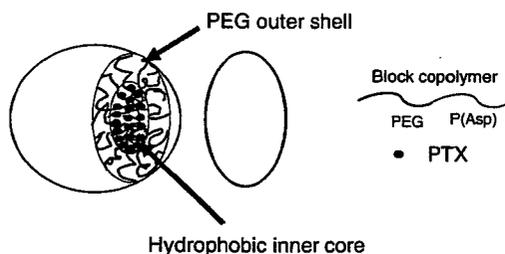

Figure 1 Schematic structure of NK105. A polymeric micelle carrier of NK105 consists of a block copolymer of PEG (molecular weight of about 12 000) and modified polyaspartate. PEG is believed to be the outer shell of the micelle. PEG is believed to form the outer shell of the micelle. NK105 has a highly hydrophobic inner core, and therefore can entrap a sufficient amount of PTX.

times the upper normal limit); normal renal function (serum creatinine $\leqslant 1.5$ mg dl^{-1}); normal cardiac function (New York Heart Association (NYHA) classification of $\leqslant 1$); normal pulmonary function (PaO$_2 \geqslant 60$ mm Hg); no chemotherapy within 4 weeks (6 weeks for nitrosourea or mitomycin C) of the administration of NK105; and a life expectancy of more than 2 months. Patients with serious infections (including hepatitis B, hepatitis C, or HIV) were ineligible for enrolment in the study. Patients who had been previously treated with a taxane were excluded because of assessing neuropathy. Patients were also excluded if they were pregnant or lactating. Additionally, any patient whom the investigators considered ineligible was excluded.

Drug administration

NK105 was dissolved in 5% glucose solution for injection at room temperature. NK105 was administered intravenously without in-line filtration and without premedication. NK105 solution was infused using an electric pump at a speed of 250 ml h^{-1}.

Dosage and dose escalation

The starting dosage of NK105 was 10 mg m^{-2}, which is one-third of the toxic dose low in dogs. NK105 was administered once every 3 weeks, and the treatment was continued unless a severe adverse event or disease progression was observed. Dose escalation was performed according to the previously described accelerated titration method (Simon et al, 1997; Matsumura et al, 2004).

Toxicity was graded from 1 to 4 using the National Cancer Institute Common Toxicity Criteria (version 2.0). Intrapatient dose escalation was not permitted. The MTD was defined as the level at which two out of six patients experienced dose-limiting toxicities (DLTs). The recommended dosage for a phase II trial was defined by the Efficacy and Safety Assessment Committee based on the safety, pharmacokinetics, and efficacy results of this trial. DLT was defined as grade 4 neutropenia lasting more than 5 days, a platelet count of less than 25 000 μl^{-1}, or grade 3 or higher non-haematological toxicity, with the exception of nausea, vomiting, appetite loss, and hypersensitivity.

Pretreatment assessment and follow-up care

A complete medical history and physical examination, performance status evaluation, complete blood cell count (CBC), blood chemistry, urinalysis, electrocardiogram (ECG), and a computed tomography (CT) examination were performed in each patient. Other examinations were performed only in the presence of a specific clinical indication. Patients were physically examined every day until the second administration of NK105; CBC and blood chemistry tests were performed on day 3 and weekly thereafter. An ECG examination was repeated before each administration of NK105. Tumour marker levels were also measured before every administration. Tumour response was evaluated according to the Response Evaluation Criteria in Solid Tumors criteria (Therasse et al, 2000).

Liquid chromatography/tandem mass spectrometry determination of PTX concentrations

The PTX concentrations determined in the present phase I study represented the total drug concentrations (both micelle-entrapped and released). It was difficult to measure released PTX and micelle-entrapped PTX separately, because the equilibrium between both forms could not keep constant during the separating procedure. PTX was extracted from human plasma (0.2 ml) or urine (0.5 ml) by deproteinisation with acetonitrile. The quantifications of PTX in plasma and urine were performed using liquid chromatography/tandem mass spectrometry. Reversed-phase column-switching

chromatography was conducted using an ODS column and detection was enabled by electrospray ionisation of positive mode.

Pharmacokinetic analysis

The following pharmacokinetic parameters were calculated for each patient using a non-compartmental model using the WinNonlin Professional version 4.1 program (Pharsight Corporation, Mountain View, CA, USA). The maximum concentration (C_{max}) was the maximum observed plasma concentration of PTX, and the time-to-the-maximum concentration (T_{max}) was the time corresponding to C_{max}. The area under the concentration (AUC)–time curve from time zero up to the last quantifiable time point (AUC_{0-t}) was calculated using the linear trapezoidal rule, and the area under the concentration–time curve from zero until infinity (AUC_{0-inf}) was calculated as the sum of AUC_{0-t} and the extrapolated area under the zero moment curve from the last quantifiable time point to infinity calculated by dividing the plasma concentration of the last quantifiable time point (observed value) by the elimination rate constant. The half-life of the terminal phase ($t_{1/2z}$) was calculated as $\log_e 2/\lambda z$, where λz is the elimination rate constant calculated from the terminal linear portion of the log of the concentration in plasma. Total clearance (CL_{tot}), the volume of distribution at steady state (V_{ss}), and renal clearance (CL_r) were calculated using the following equations, where D is the dose and $AUMC_{inf}$ the area under the first moment curve from time zero until infinity:

$$CL_{tot} = D/AUC_{inf}$$

$$V_{ss} = AUMC_{inf}/AUC_{inf} \times CL_{tot}$$

$$CL_r = \text{cumulative urinary excretion}/AUC_{inf}$$
$$/\text{body surface area}$$

RESULTS

Patient characteristics

Nineteen eligible patients were recruited for the study (Table 1). All the patients had received chemotherapy before enrolment. Prior therapies ranged from 1 to 3 regimens of chemotherapy. None of the patients had received taxane chemotherapy. All the patients were included in the safety and response analyses.

Dosing

Dosage escalation started at $10\,\text{mg}\,\text{m}^{-2}$ and was increased up to $180\,\text{mg}\,\text{m}^{-2}$. In total, 73 administrations were performed in 19 patients. Eighteen patients received more than two administra-

Table 1 Patient characteristics

Number of patients	19
Male/female	13/6
Age (years)	
Median	57
Range	43–72
ECOG PS	
Median	0
0	10
1	9
Prior treatment	
Chemotherapy regimens	
Median	1
Range	1–3

tions. The maximum number of treatments was 14 courses at $150\,\text{mg}\,\text{m}^{-2}$; the average number of administrations at all levels was 3.8 courses. Up until $80\,\text{mg}\,\text{m}^{-2}$, grade 2 toxicity was not observed during the first course.

According to the original protocol, the dosage of NK105 should have been doubled for each escalation until grade 2 toxicity. However, the safety committee recommended that the dosage should be raised by 40% instead of 100% at $110\,\text{mg}\,\text{m}^{-2}$ and that a modified Fibonacci escalation method should be implemented. Therefore, we recruited three patients at dosage level 5 ($110\,\text{mg}\,\text{m}^{-2}$) and re-started the dose identification study using a modified Fibonacci method.

Haematological toxicity

Significant myelosuppression was not observed up to level 4 ($80\,\text{mg}\,\text{m}^{-2}$). At level 7 ($180\,\text{mg}\,\text{m}^{-2}$), two out of five patients appeared to have acquired DLTs, namely grade 4 neutropenia lasting for more than 5 days. On the basis of these results, $180\,\text{mg}\,\text{m}^{-2}$ was considered to be the MTD, with neutropenia as the DLT. Since a dosage of $150\,\text{mg}\,\text{m}^{-2}$ was considered to be the recommended dosage for phase II studies, an additional four patients were enrolled at a dosage of $150\,\text{mg}\,\text{m}^{-2}$; one patient developed DLT, namely grade 4 neutropenia lasting for more than 5 days (Table 2). During the entire period of this study, G-CSF was never used to rescue patients.

Nonhaematological toxicity

The NK105 injection was generally uneventful and well tolerated in terms of nonhaematological toxicities (Table 2). Most of the toxicities were grade 1; none of the patients manifested grade 4 toxicity. A few patients developed a grade 1 elevation in AST or ALT, but these changes were transient. Pain or local toxicity in the area of the injection was not observed in any of the patients treated with NK105. No infusion-related reactions were observed; such reactions sometimes occur during liposomal drug administration. Patients were not premedicated with steroids or antihistamines. Only one patient at $180\,\text{mg}\,\text{m}^{-2}$ developed grade 2 hypersensitivity. After the first course, the patient received premedication of hydrocortisone and did not develop such hypersensitivity after that. The other 18 patients did not experience any hypersensitivity during the study. Neuropathy occurred in a typical stocking/glove distribution and was manifested by numbness. Three patients at level 6 ($150\,\text{mg}\,\text{m}^{-2}$) and three patients at level 7 ($180\,\text{mg}\,\text{m}^{-2}$) experienced grade 1 neurotoxicity during 1 cycle. Of the four patients who received multicycle treatment more than five times, only three patients developed grade 2 neuropathy and the other patient developed grade 1 neuropathy. Even one patient who received 14 cycles of treatment experienced only grade 2 neuropathy.

Pharmacokinetics

The plasma concentrations of PTX after the intravenous infusion of NK105 were determined in each of the patients enrolled at a dose of $150\,\text{mg}\,\text{m}^{-2}$ (Figure 2A). The C_{max} (Figure 2B) and AUC (Figure 2C) increased as the doses were escalated from 10 to $180\,\text{mg}\,\text{m}^{-2}$. The pharmacokinetic parameters are summarised in Table 3. The $t_{1/2z}$ ranged from 7.0 to 13.2 h, and a slight tendency towards a dose-dependent extension of this parameter was observed. The CL_{tot} ranged from 280.9 to $880.4\,\text{ml}\,\text{h}^{-1}\,\text{m}^{-2}$, and the V_{ss} ranged from 3668.9 to $10\,400.3\,\text{ml}\,\text{m}^{-2}$. Although these parameters were slightly reduced depending on the dose, linear pharmacokinetics was assumed to have been observed in the dose range from 10 to $180\,\text{mg}\,\text{m}^{-2}$. The AUC of NK105 at $150\,\text{mg}\,\text{m}^{-2}$ (recommended phase II dose) was about 15-fold larger than that of conventional PTX at dose of $210\,\text{mg}\,\text{m}^{-2}$ (conventional dose for a

Table 2 Haematological and nonhaematological toxicities (cycle I and all cycles)

	10–110 mg m⁻² (n = 7) grade				150 mg m⁻² (n = 7) grade				180 mg m⁻² (n = 7) grade			
	1	2	3	4	1	2	3	4	1	2	3	4
Cycle I												
Leukopenia	2	0	2	0	1	5	1	0	1	1	3	0
Neutropenia	1	0	1	1	0	2	1	3[a]	0	0	3	2[b]
Thrombocytopenia	1	0	0	0	2	0	0	0	4	0	0	0
Hemoglobin	1	0	0	0	2	2	0	0	1	0	0	0
Neuropathy	0	0	0	0	3	0	0	0	3	0	0	0
Myalgia	1	0	0	0	3	0	0	0	2	1	0	0
Arthralgia	1	0	0	0	4	0	0	0	3	0	0	0
Hypersensitivity	0	0	0	0	0	0	0	0	0	1	0	0
Rash	1	0	0	0	1	3	0	0	4	0	0	0
Fatigue	1	0	0	0	5	0	0	0	4	0	0	0
Fever	2	0	0	0	2	0	0	0	1	0	1	0
Anorexia	0	0	0	0	3	0	0	0	1	0	0	0
Nausea	1	0	0	0	1	0	0	0	1	0	0	0
Stomatitis	0	0	0	0	1	0	0	0	1	0	0	0
Alopecia	3	0	—	—	5	0	—	—	5	0	—	—
All cycles												
Leukopenia	3	0	2	0	1	4	2	0	1	1	3	0
Neutropenia	1	0	1	1	1	1	1	4	0	0	3	2
Thrombocytopenia	1	0	0	0	3	0	0	0	4	0	0	0
Hemoglobin	1	0	0	0	1	5	0	0	1	0	0	0
Neuropathy	2	0	0	0	1	3	0	0	4	0	0	0
Myalgia	1	1	0	0	3	0	0	0	2	1	0	0
Arthralgia	2	0	0	0	4	0	0	0	3	0	0	0
Hypersensitivity	0	0	0	0	0	0	0	0	0	1	0	0
Rash	1	0	0	0	3	3	0	0	4	0	0	0
Fatigue	3	0	0	0	5	1	0	0	4	0	0	0
Fever	3	0	0	0	3	1	0	0	1	0	1	0
Anorexia	2	1	0	0	2	1	0	0	2	0	0	0
Nausea	1	0	0	0	1	0	0	0	2	0	0	0
Stomatitis	1	0	0	0	2	0	0	0	1	0	0	0
Alopecia	2	2	—	—	4	3	—	—	4	1	—	—

[a]One of three patients developed DLT, namely grade 4 neutropenia lasting for more than 5 days. [b]These two patients developed DLT, namely grade 4 neutropenia lasting for more than 5 days.

3-week regimen in Japanese patients) (Tamura *et al*, 1995). The V_{ss} and CL_{tot} of NK105 were significantly lower than those of conventional PTX. .

The cumulative urinary excretion rates of PTX (0–73 h) after the administration of NK105 were 2.8–9.2%. These values were low, similar to those reported after the administration of conventional PTX (Tamura *et al*, 1995). The CL_r ranged from 11.7 to 66.4 ml h⁻¹ m⁻³, and was slightly decreased with the dose. Since the ratio of CL_r to CL_{tot} was 3–9%, CL_r hardly contributed to CL_{tot}.

Therapeutic response

Six patients (two gastric, two bile duct, one colon, and one pancreatic) were evaluated as having had a stable disease for longer than 4 weeks at the time of the study's completion. A partial response was seen in a patient with metastatic pancreatic cancer who had been treated at 150 mg m⁻², and in whom the size of the liver metastasis had decreased by more than 90%, compared to the baseline scan (Figure 3A). This patient had previously undergone treatment with gemcitabine. The antitumour response was maintained for nearly 1 year. In a patient with stomach cancer who was treated at 150 mg m⁻², about 40% reduction was observed in a peritoneal metastasis, but a liver metastasis remained stable (Figure 3B).

DISCUSSION

The observed toxicities of NK105 were similar to those expected for conventional PTX. The DLT was neutropenia. The recom-

mended phase II dose using a 3-week schedule was determined to be 150 mg m⁻². This recommended dose of NK105 is less than that of conventional PTX (210 mg m⁻²). Since the plasma AUC of the recommended dose of NK105 was 15- to 20-fold higher than that of the recommended dose of conventional PTX (210 mg m⁻²), whether the so-called therapeutic window of NK105 is wider than that of conventional PTX should be determined in a future phases II or III trial, although the therapeutic window of NK105 appears to be wider than that of free PTX in mice experiments (Hamaguchi *et al*, 2005).

In general, haematological toxicity was mild and well managed in this trial. PTX is known to cause cumulative peripheral neuropathy resulting in the discontinuation of treatment with PTX. At a dose of 150 mg m⁻², three out of seven patients experienced only grade 1 neuropathy during the first cycle. Since the patients enrolled in this trial had almost intractable cancer, such as pancreatic or stomach, a relatively small number of patients received multiple cycles of treatment. Therefore, NK105-related neurotoxicity could not be evaluated in this study. However, three out of four patients who received more than five cycles of treatment experienced transient grade 2 peripheral neuropathy, and other patient developed transient grade 1 peripheral neuropathy. Future phase II trials may clarify whether NK105 is less toxic in terms of peripheral neuropathy when compared with conventional PTX, Abraxane, and other PTX compounds. Another characteristic adverse effect of PTX is hypersensitivity, which may be mainly caused by Cremophor EL. Since NK105 is not formulated in a Cremophor EL-containing solvent, we presumed that hypersensitivity would be diminished.
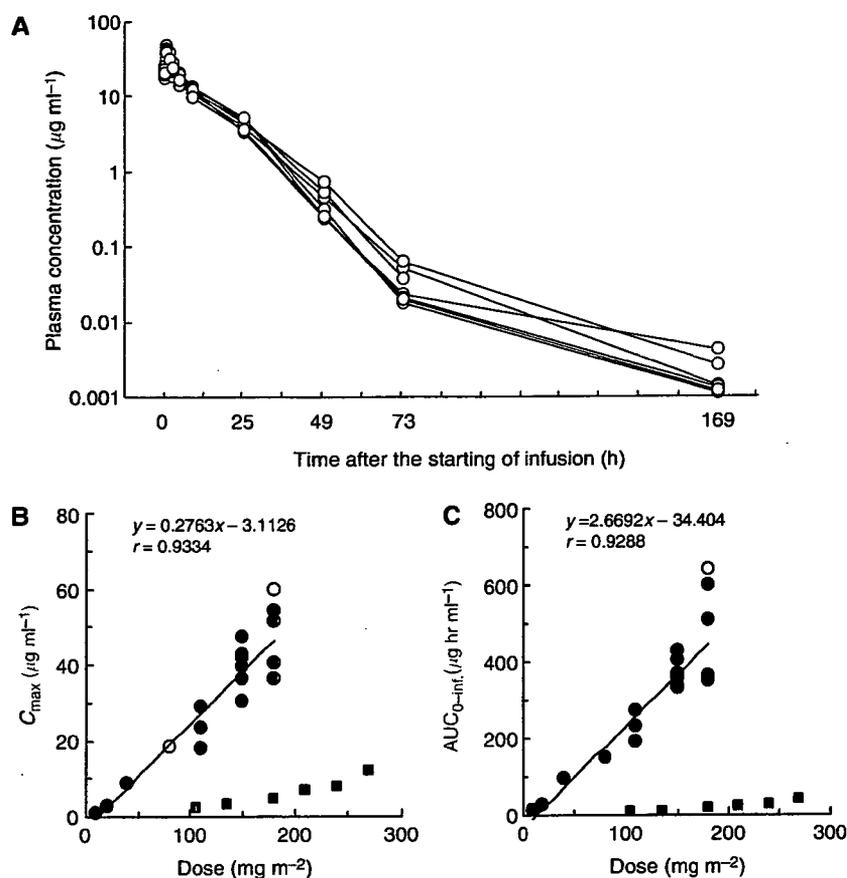
Figure 2 (**A**) Individual plasma concentrations of PTX in seven patients following 1-h intravenous infusion of NK105 at a dose of $150\,\mathrm{mg\,m^{-2}}$. (**B**) Relationships between dose and C_{max} and (**C**) between dose and $AUC_{0-inf.}$ of PTX in patients following 1-h intravenous infusion of NK105. Regression analysis for dose vs C_{max} was applied using all points except one patient at $80\,\mathrm{mg\,m^{-2}}$ whose medication time became 11 min longer and one patient at $180\,\mathrm{mg\,m^{-2}}$ who had medication discontinuation and steroid medication. (Plots were shown as open circle). Regression analysis for dose vs $AUC_{0-inf.}$ was applied using all points except one patient who had medication discontinuation and steroid medication. (Plot was shown as open circle.) Relationships between dose and C_{max}, and $AUC_{0-inf.}$ in patients following conventional PTX administration were plotted (closed square, see Tamura et al, 1995).

Table 3 Pharmacokinetic parameters

	Dose ($\mathrm{mg\,m^{-2}}$)	n	C_{max} ($\mu\mathrm{g\,ml^{-1}}$)	$AUC_{0-inf.}$ ($\mu\mathrm{g\,h\,ml^{-1}}$)	$t_{1/2}$ (h)	CL_{tot} ($\mathrm{ml\,h^{-1}\,m^{-2}}$)	V_{ss} ($\mathrm{ml\,m^{-2}}$)	UE^a (%)	CL_r ($\mathrm{ml\,h\,m^{-2}}$)
NK105	10	1	0.9797	11.4	9	880.4	10400.3	7.5	66.4
	20	1	2.8971	29.1	8.5	687.9	8027	8.6	59.4
	40	1	8.8334	93.9	13.2	426.1	5389.8	5.2	22
	80	1	18.4533	149.3	7	535.8	5875.8	4.7	25.3
	110	3	23.3924	232	9.7	483.3	5881.2	7.6	35.6
			±5.6325	±39.1	±1.6	±82.7	±1512.0	±1.7	±6.9
	150	7	40.1699	369.8	10.6	408.6	4527.1	5.3	21.6
			±5.5334	±35.2	±1.3	±37.3	±639.5	±1.5	±6.5
	180	4^b	45.6278	454.5	11.3	416.5	4983.4	5.9	23.7
			±8.6430	±119.1	±0.6	±104.7	±887.5	±1.4	±4.2

^{a}UE, urinary excretion. ^{b}One patient at $180\,\mathrm{mg\,m^{-2}}$ level was omitted from the calculation of summary pharmacokinetic parameters, as there was administrating interruption for developing allergic reactions.

Indeed, the results of this clinical trial show that NK105 can be administered safely as a short infusion (1 h) without the administration of antiallergic agents like dexamethasone and antihistamine, although one patient at $180\,\mathrm{mg\,m^{-2}}$ developed transient grade 2 hypersensitivity at the first course. Therefore, NK105 may offer advantages in terms of safety and patient convenience and comfort.

The pharmacokinetic analysis of NK105 suggests that the distribution of PTX-incorporating micelles is mostly restricted to the plasma and, in part, to extracellular fluids in the body. This is consistent with data obtained in a preclinical study (Hamaguchi et al, 2005) showing that the distribution of NK105 in tissues is characterised by an EPR effect, similar to that of tumour and inflammatory lesions, or by the presence of a reticuloendothelial
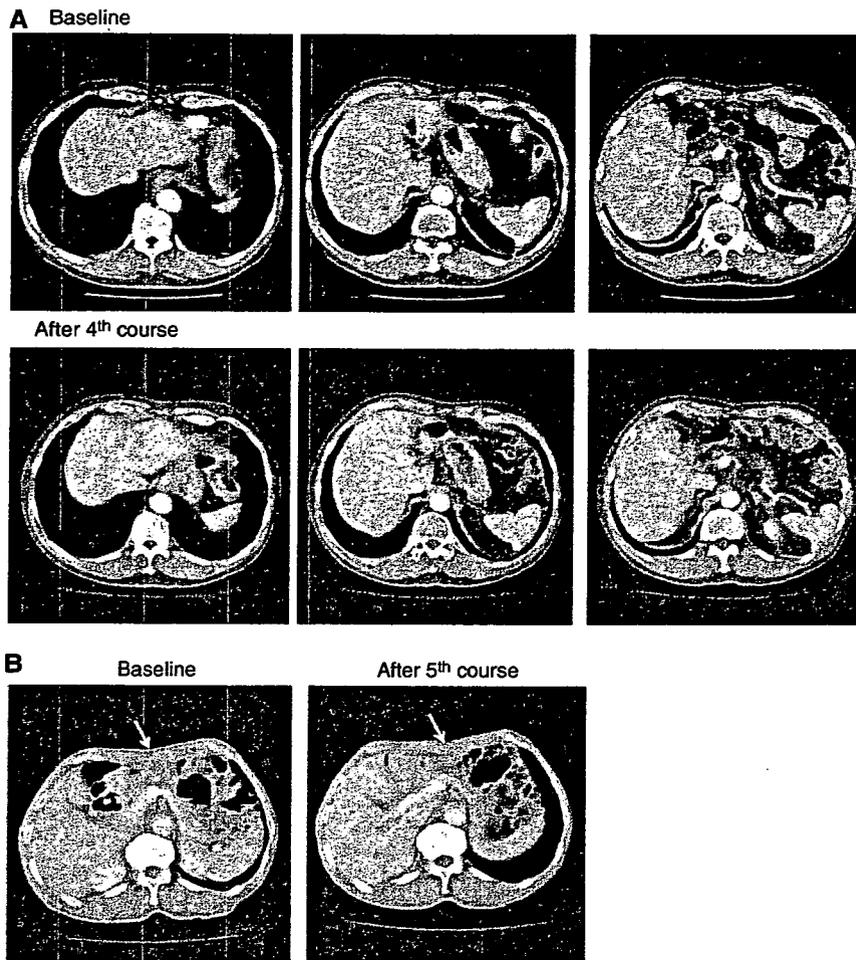
A Baseline

After 4th course

B   Baseline   After 5th course

Figure 3 Serial CT scans. (**A**) A 60-year-old male with pancreatic cancer who was treated with NK105 at a dose level of 150 mg m^{-2}. Baseline scan (upper panels) showing multiple metastasis in the liver. Partial response, characterized by a more than 90% decrease in the size of the liver metastasis (lower panels) compared with the baseline scan. The antitumour response was maintained for nearly 1 year. (**B**) A 64-year-old male with stomach cancer who was treated with NK105 at a dose level of 150 mg m^{-2}. Baseline scan (left panel) showing a peritoneal metastasis and liver metastasis. About 40% reduction (right panel) was observed in peritoneal metastasis, but not in the liver metastasis after fifth course.

Table 4 Pharmacokinetic parameters

	Dose (mg m^{-2})	n	C_{max} (μg ml^{-1})	AUC$_{0\ inf.}$ (μg h^{-1} ml^{-1})	$t_{1/2}$ (h)	CL$_{tot}$ (ml h^{-1} m^{-2})	V_{ss} (ml m^{-2})	UE (%)	CL$_r$ (ml h m^{-2})
NK105	150	7	40.1699	369.8	10.6	408.6	4527.1	5.3	21.6
			±5.5334	±35.2	±1.3	±37.3	±639.5	±1.5	±6.5
PTX	210	5	6.744	23.18	13.3	10740	58900	9.45	1020
			±2.733	±10.66	±1.5	±4860	±24700	±3.76	±648
XYOTAX[a]	233	4	NA	1583	120	276	6200	NA	NA
				±572	±28	±63	±2100		
Abraxane	300	5	13.52	17.61	14.6	17700	370000	NA	NA
			±0.95	±3.70	±2.04	±3894	±85100		
Genoxol-PM	300	3	3.107	11.58	11.4	29300	NA	NA	NA
			±1.476	±4.28	±2.4	±13800			

[a]Conjugated taxanes.

system. When compared with conventional PTX at a dose of 210 mg m^{-2} (conventional dose for a 3-week regimen in Japanese patients), NK105 at a dose of 150 mg m^{-2} (recommended phase II dose) exhibited more than 15-fold larger plasma AUC and a 26-fold lower CL$_{tot}$. The larger plasma AUC is consistent with the stability of the micelle formulation in plasma. The V_{ss} of NK105

was 13-fold lower than that of conventional PTX. This suggests that PTX may have a relatively lower distribution in normal tissue, including normal neural tissue, following NK105 administration. Regarding the drug distribution in tumours, nanoparticle drug carriers have been known to preferentially accumulate in tumour tissues utilising the EPR effect (Matsumura and Maeda, 1986;

Maeda et al, 2000; Duncan, 2003). We speculate that NK105 accumulates more in tumour tissues than free PTX, since NK105 is very stable in the circulation and exhibits a markedly higher plasma AUC than free PTX. Moreover, a polymeric micelle carrier system for a drug has the potential to enable the sustained release of the drug inside a tumour following the accumulation of micelles in the tumour tissue (Hamaguchi et al, 2005; Uchino et al, 2005; Koizumi et al, 2006). Regarding NK105 in particular, this sustained release may begin at a PTX-equivalent dose of $<1\,\mu g\,ml^{-1}$ (data not shown). Consequently, the released PTX is distributed throughout the tumour tissue where it kills the cancer cells directly.

In the present study, NK105 appeared to exhibit characteristic pharmacokinetics different from those of other PTX formulations including conventional PTX, Abraxane, Genexol-PM, and Xyotax. For example, previous clinical PK data at each phase II

recommended dose shown that plasma AUC and C_{max} were 11.58 and 3.1 in Genexol-PM (Table 4). The antitumour activities seen in two patients with intractable cancers are encouraging. In addition, we recently demonstrated in preclinical study that combined NK105 chemotherapy with radiation exerts a significantly more potent antitumour activity, compared with combined PTX therapy and radiation (Negishi et al, 2006). This data on NK105 justifies its continued clinical evaluation.

ACKNOWLEDGEMENTS

REFERENCES

Boddy AV, Plummer ER, Todd R, Sludden J, Griffin M, Robson L, Cassidy J, Bissett D, Bernareggi A, Verrill MW, Calvert AH (2005) A phase I and pharmacokinetic study of paclitaxel poliglumex (XYOTAX), investigating both 3-weekly and 2-weekly schedules. Clin Cancer Res 11: 7834–7840

Carney DN (1996) Chemotherapy in the management of patients with inoperable non-small cell lung cancer. Semin Oncol 23: 71–75

Crown J, O'Leary M (2000) The taxanes: an update. Lancet 355: 1176–1178

Deisai N, Trieu V, Yao R (2003) Evidence of greater antitumor activity of Cremophor-free nanoparticle albumin-bound (nab) paclitaxel (Abraxane) compared with Taxol, role of a novel albumin transporter mechanism. 26th Annual San Antonio Breast Cancer Symposium San Antonio, TX

Duncan R (2003) The dawning era of polymer therapeutics. Nat Rev Drug Discov 2: 347–360

Gradishar WJ, Tjulandin S, Davidson N, Shaw H, Desai N, Bhar P, Hawkins M, O'Shaughnessy J (2005) Phase III trial of nanoparticle albumin-bound paclitaxel compared with polyethylated castor oil-based paclitaxel in women with breast cancer. J Clin Oncol 23: 7794–7803

Hamaguchi T, Matsumura Y, Suzuki M, Shimizu K, Goda R, Nakamura I, Nakatomi I, Yokoyama M, Kataoka K, Kakizoe T (2005) NK105, a paclitaxel-incorporating micellar nanoparticle formulation, can extend in vivo antitumour activity and reduce the neurotoxicity of paclitaxel. Br J Cancer 92: 1240–1246

Ibrahim NK, Desai N, Legha S, Soon-Shiong P, Theriault RL, Rivera E, Esmaeli B, Ring SE, Bedikian A, Hortobagyi GN, Ellerhorst JA (2002) Phase I and pharmacokinetic study of ABI-007, a Cremophor-free, protein-stabilized, nanoparticle formulation of paclitaxel. Clin Cancer Res 8: 1038–1044

Kim TY, Kim DW, Chung JY, Shin SG, Kim SC, Heo DS, Kim NK, Bang YJ (2004) Phase I and pharmacokinetic study of Genexol-PM, a cremophor-free, polymeric micelle-formulated paclitaxel, in patients with advanced malignancies. Clin Cancer Res 10: 3708–3716

Kloover JS, den Bakker MA, Gelderblom H, van Meerbeeck JP (2004) Fatal outcome of a hypersensitivity reaction to paclitaxel: a critical review of premedication regimens. Br J Cancer 90: 304–305

Koizumi F, Kitagawa M, Negishi T, Onda T, Matsumoto S, Hamaguchi T, Matsumura Y (2006) Novel SN-38-incorporating polymeric micelles, NK012, eradicate vascular endothelial growth factor-secreting bulky tumors. Cancer Res 66: 10048–10056

Maeda H, Wu J, Sawa T, Matsumura Y, Hori K (2000) Tumor vascular permeability and the EPR effect in macromolecular therapeutics: a review. J Control Release 65: 271–284

Matsumura Y, Maeda H (1986) A new concept for macromolecular therapeutics in cancer chemotherapy: mechanism of tumoritropic accumulation of proteins and the antitumor agent smancs. Cancer Res 46: 6387–6392

Matsumura Y, Hamaguchi T, Ura T, Muro K, Yamada Y, Shimada Y, Shirao K, Okusaka T, Ueno H, Ikeda M, Watanabe N (2004) Phase I clinical trial and pharmacokinetic evaluation of NK911, a micelle-encapsulated doxorubicin. Br J Cancer 91: 1775–1781

Negishi T, Koizumi F, Uchino H, Kuroda J, Kawaguchi T, Naito S, Matsumura Y (2006) NK105, a paclitaxel-incorporating micellar nanoparticle, is a more potent radiosensitising agent compared to free paclitaxel. Br J Cancer 95: 601–606

Nyman DW, Campbell KJ, Hersh E, Long K, Richardson K, Trieu V, Desai N, Hawkins MJ, Von Hoff DD (2005) Phase I and pharmacokinetics trial of ABI-007, a novel nanoparticle formulation of paclitaxel in patients with advanced nonhematologic malignancies. J Clin Oncol 23: 7785–7793

Rowinsky EK, Donehower RC (1995) Paclitaxel (taxol). New Engl J Med 332: 1004–1014

Rowinsky EK, Cazenave LA, Donehower RC (1990) Taxol: a novel investigational antimicrotubule agent. J Natl Cancer Inst 82: 1247–1259

Simon R, Freidlin B, Rubinstein L, Arbuck SG, Collins J, Christian MC (1997) Accelerated titration designs for phase I clinical trials in oncology. J Natl Cancer Inst 89: 1138–1147

Singer JW, Baker B, De Vries P, Kumar A, Shaffer S, Vawter E, Bolton M, Garzone P (2003) Poly-(L)-glutamic acid-paclitaxel (CT-2103) [XYO-TAX], a biodegradable polymeric drug conjugate: characterization, preclinical pharmacology, and preliminary clinical data. Adv Exp Med Biol 519: 81–99

Tamura T, Sasaki Y, Nishiwaki Y, Saijo N (1995) Phase I study of paclitaxel by three-hour infusion: hypotension just after infusion is one of the major dose-limiting toxicities. Jpn J Cancer Res 86: 1203–1209

Therasse P, Arbuck SG, Eisenhauer EA, Wanders J, Kaplan RS, Rubinstein L, Verweij J, Van Glabbeke M, van Oosterom AT, Christian MC, Gwyther SG (2000) New guidelines to evaluate the response to treatment in solid tumors. European Organization for Research and Treatment of Cancer, National Cancer Institute of the United States, National Cancer Institute of Canada. J Natl Cancer Inst 92: 205–216

Uchino H, Matsumura Y, Negishi T, Koizumi F, Hayashi T, Honda T, Nishiyama N, Kataoka K, Naito S, Kakizoe T (2005) Cisplatin-incorporating polymeric micelles (NC-6004) can reduce nephrotoxicity and neurotoxicity of cisplatin in rats. Br J Cancer 93: 678–687

Weiss RB, Donehower RC, Wiernik PH, Ohnuma T, Gralla RJ, Trump DL, Baker Jr JR, Van Echo DA, Von Hoff DD, Leyland-Jones B (1990) Hypersensitivity reactions from taxol. J Clin Oncol 8: 1263–1268

– 619 –

Irinotecan pharmacokinetics/pharmacodynamics and *UGT1A* genetic polymorphisms in Japanese: roles of *UGT1A1*6* and *28*

Hironobu Minami[a], Kimie Sai[b,c], Mayumi Saeki[b], Yoshiro Saito[b,d], Shogo Ozawa[b,e], Kazuhiro Suzuki[c], Nahoko Kaniwa[b,f], Jun-ichi Sawada[b,d], Tetsuya Hamaguchi[g], Noboru Yamamoto[g], Kuniaki Shirao[g], Yasuhide Yamada[g], Hironobu Ohmatsu[h], Kaoru Kubota[h], Teruhiko Yoshida[i], Atsushi Ohtsu[j] and Nagahiro Saijo[k]

Objectives SN-38, an active metabolite of irinotecan, is detoxified by glucuronidation with UGT1A isoforms, 1A1, 1A7, 1A9, and 1A10. The pharmacogenetic information on *UGT1A* haplotypes covering all these isoforms is important for the individualized therapy of irinotecan. Associations between *UGT1A* haplotypes and pharmacokinetics/ pharmacodynamics of irinotecan were investigated to identify pharmacogenetic markers.

Methods Associations between *UGT1A* haplotypes and the area under concentration curve ratio (SN-38 glucuronide/ SN-38) or toxicities were analyzed in 177 Japanese cancer patients treated with irinotecan as a single agent or in combination chemotherapy. For association analysis, diplotypes of *UGT1A* gene segments [(*1A1, 1A7, 1A9, 1A10*), and Block C (common exons 2–5)] and combinatorial haplotypes (*1A9-1A7-1A1*) were used. The relationship between diplotypes and toxicities was investigated in 55 patients treated with irinotecan as a single agent.

Results Among diplotypes of *UGT1A* genes, patients with the haplotypes harboring *UGT1A1*6* or *28* had significantly reduced area under concentration curve ratios, with the effects of *UGT1A1*6* or *28* being of a similar scale. A gene dose effect on the area under concentration curve ratio was observed for the number of haplotypes containing *28* or *6* (5.55, 3.62, and 2.07 for 0, 1, and 2 haplotypes, respectively, *P*<0.0001). In multivariate

analysis, the homozygotes and double heterozygotes of *6* and *28* (*6/*6, *28/*28 and *6/*28) were significantly associated with severe neutropenia in 53 patients who received irinotecan monotherapy.

Conclusions The haplotypes significantly associated with reduced area under concentration curve ratios and neutropenia contained *UGT1A1*6* or *28*, and both of them should be genotyped before irinotecan is given to Japanese and probably other Asian patients. *Pharmacogenetics and Genomics* 17:497–504 © 2007 Lippincott Williams & Wilkins.

[a]Division of Oncology/Hematology, National Cancer Center Hospital East, Kashiwa, [b]Project Team for Pharmacogenetics, [c]Division of Biosignaling, [d]Division of Biochemistry and Immunochemistry, [e]Division of Pharmacology, [f]Division of Medicinal Safety Science, National Institute of Health Sciences, [g]Division of Internal Medicine, National Cancer Center Hospital, [h]Division of Thoracic Oncology, National Cancer Center Hospital East, Kashiwa, [i]Genetics Division, National Cancer Center Research Institute, Tokyo, [j]Division of Gastrointestinal Oncology/Digestive Endoscopy and [k]National Cancer Center Hospital East, Kashiwa, Japan.

Correspondence to Hironobu Minami, MD, Head and Chair, Division of Oncology/Hematology, National Cancer Center Hospital East, 6-5-1 Kashiwanoha, Kashiwa 277-8577, Japan
Tel: +81471331111; e-mail: hminami@east.ncc.go.jp

Introduction

Irinotecan, an anticancer prodrug, is widely applied for colorectal, lung, stomach, ovarian, and other various cancers. It is activated by carboxylesterases to SN-38 (7-ethyl-10-hydroxycamptothecin), which shows antitumor activity by inhibiting topoisomerase I [1,2]. SN-38 is subsequently glucuronidated by uridine diphosphate glucuronosyltransferases (*UGTs*) to form an inactive metabolite, SN-38 glucuronide (SN-38G) [3]. Dose-limiting toxicities of irinotecan are diarrhea and leukopenia [4], and reduced activity for SN-38G formation is closely related to severe toxicities [5]. Among UGT

isoforms, UGT1A1 is abundant in both the liver and intestine and is thought to be mainly responsible for inactivation of SN-38 [3,6]. Genetic polymorphisms of *UGT1A1* result in reduced enzyme activity and increased toxicity by irinotecan. A significant association of *UGT 1A1*28*, a repeat polymorphism of the TATA box (-40_-39insTA) [3,7], with severe irinotecan-induced diarrhea/leukopenia was first reported in a retrospective study of Japanese cancer patients [8]. Subsequent pharmacogenetic studies in Caucasians have shown close associations of *28* with reduced glucuronidation of SN-38 and/or severe neutropenia/diarrhea [9–12]. These

studies have clearly indicated that *28 is a good genetic marker for individualized irinotecan therapy. On the basis of these observations, the Food and Drug Administration of the United States has approved an amendment of the label for Camptosar (irinotecan HCl) and added a warning to consider a reduction in the starting dose of irinotecan for *28 homozygous patients (NDA 20-571/S-024/S-027/S-028).

There is significant racial difference in *UGT1A1* polymorphisms among Asians, Caucasians, and Africans [13]. Although the association of *UGT 1A1*28* with toxicities by irinotecan was first described in Japanese patients, its frequency in Japanese is one-third of that in Caucasians. Another low-activity allele *6 [211G > A(G71R)], which is not detected in Caucasians or Africans, is as frequent as the *28 allele in Japanese. Moreover, the area under concentration curve (AUC) ratio of SN-38G to SN-38 was decreased in patients having *6 haplotypes [14].

In addition to UGT1A1, recent studies have suggested possible contributions to SN-38G formation by UGT1A7, 1A9, and 1A10 [15–17], which are expressed in the gastrointestinal tract, the liver and intestine, and extrahepatic tissues, respectively [18]. Altered activity resulted from genetic polymorphisms of these isoforms, including *1A7*3* [387T > G(N129K), 391C > A(R131K), 622T >C(W208R)], *1A9*22* (-126_-118T$_9$ > T$_{10}$), *1A9*5* [766G >A(D256N)], and *UGT1A10*3* [605C > T(T202I)], but clinical relevance of these polymorphisms is yet to be elucidated [16,19–24]. Moreover, close linkages among *1A9*, *1A7*, and *1A1* polymorphisms were found in Caucasians and Asians in an ethnic-specific manner [20,25–27]. Therefore, comprehensive investigation that covers these genes, along with linkages among the polymorphisms, is needed, in each ethnic population, to evaluate associations between the genetic polymorphisms and pharmacokinetics, as well as clinical outcomes of irinotecan therapy.

Recently, we have analyzed the segmental and block haplotypes of *1A8*, *1A10*, *1A9*, *1A7*, *1A6*, *1A4*, *1A3* and *1A1*, and the common exons 2–5 (Block C) in a Japanese population, including the 177 cancer patients treated with irinotecan, and showed close linkages between the haplotypes, that is, *1A9*22* and *1A7*1*, *1A7*3* and *1A1*6*, and *1A7*3* and *1A1*28* [28]. Preliminary results of *UGT1A1* pharmacogenetics on 85 of these cancer patients were reported previously [14]. In the current study, we investigated the pharmacogenetics of irinotecan, focusing on diplotypes of the *UGT1A* complex covering *1A1*, *1A7*, *1A9*, *1A10*, and Block C (exons 2–5) of 177 patients, so as to elucidate haplotypes or genetic markers associated with altered glucuronidation of SN-38 and toxicities.

Methods

Patients and treatment schedule

Patients with cancers who started chemotherapy with irinotecan at two National Cancer Center Hospitals (Tokyo and Kashiwa, Japan) were eligible if they had not received irinotecan previously. Other eligibility criteria included bilirubin ≤ 2 mg/dl, aspartate aminotransferase (GOT) ≤ 105 IU/l, alanine aminotransferase (GPT) ≤ 120 IU/l, creatinine ≤ 1.5 mg/dl, white blood cell count ≥ 3000/μl, performance status of 0–2, and at least 4 weeks after the last chemotherapy (2 weeks for radiotherapy). Exclusion criteria were diarrhea, active infection, intestinal paralysis or obstruction, and interstitial pneumonitis. The ethics committees of the National Cancer Center and the National Institute of Health Sciences approved this study, and written informed consent was obtained from all participants.

Irinotecan was administered as a single agent or in combination chemotherapy at the discretion of attending physicians. Doses and schedules were according to approved usage in Japan; intravenous 90-min infusion at a dose of 100 mg/m^2 weekly or 150 mg/m^2 biweekly. In terms of combination chemotherapy, the dose of irinotecan was reduced according to clinical protocols.

Genetic polymorphisms of UGT1As and pharmacokinetics

Detailed assay methods for genotypes of the *UGT1A* gene complex were reported previously [14,28]. In this study, we focused on the genetic variations in *UGT1A1*, *1A7*, *1A9*, and *1A10* and common exons 2–5, as they have been reported to contribute to the SN-38 glucuronidation. Haplotype analysis covering these regions was performed in our previous study [28], and haplotypes of each *UGT1A* segment [exon 1 for *1A1*, *1A7*, *1A9*, or *1A10*; and Block C (common exons 2–5)] are summarized in Fig. 1.

Pharmacokinetic analysis for irinotecan was performed as described previously [14]. Briefly, heparinized blood was collected before administration of irinotecan, as well as 0 and 20 min, and 1, 2, 4, 8, and 24 h after termination of the first infusion of irinotecan. Plasma concentrations of irinotecan, SN-38 and SN-38G were determined by the high-performance liquid chromatography [29], and AUC was calculated by the trapezoidal method using WinNonlin version 4.01 (Pharsight Corporation, Mountain View, California, USA). Associations between genotypes and the AUC ratio (AUC of SN-38G/AUC of SN-38) were evaluated in 176 patients.

Monitoring and toxicities

A complete medical history and data on physical examinations were recorded before the irinotecan therapy. Complete blood cell counts with differentials and platelet counts, as well as blood chemistry, were measured once a week during the first 2 months of irinotecan treatment. Toxicities were graded according to the Common Toxicity Criteria of National Cancer Institute version 2. Association of genetic factors with irinotecan toxicities was analyzed primarily in patients who received irinotecan as a single agent.

Fig. 1

UGT1A1

Region	Enhancer	Promoter	Exon 1		Frequency
Nucleotide change	-3279 T>G	-40_-39 insTA	211 G>A	686 C>A	
Amino acid change			G71R	P229Q	Frequency
Marker allele	*60	*28	*6	*27	

Haplotype						Frequency
	*1					0.548
	*6					0.167
	*60					0.147
*28	*28b					0.138
	*28c					
	*28d					

UGT1A10

Region	Exon 1				Frequency
Nucleotide change	4 G>A	177 G>A	200 A>G	605 C>T	
Amino acid change	A2T	M59I	E67G	T202I	Frequency
Marker allele	*2T	*2	*67G	*3	

Haplotype						Frequency
	*1					0.981
	*2					0.006
	*2T					0.003
	*3					0.010
	*67G					0.000

UGT1A7

Region	Exon 1				Frequency
Nucleotide change	387 T>G	391C>A	392 G>A	622 T>C	
Amino acid change	N129K	R131K		W208R	Frequency
Marker allele	*2,*3	*2,*3	*2,*3	*3,*4	

Haplotype						Frequency
	*1					0.630
	*2					0.147
	*3					0.223

Block C

Region	Exon.4	Exon.5		3'-UTR			Frequency
Nucleotide change	1091 C>T	1456 T>G	1598 A>C	*211(1813) C>T	*339(1941) C>G	*440(2042) C>G	
Amino acid change	P364L	Y486D	H533P				Frequency
Marker allele	*364L	*7	*533P	*IB	*IB	*IB	

Haplotypes								Frequency
	*IA							0.864
*IB	*Ib–*Ij							0.127
	*533P							
	*7							0.003
	*364L							0.006

UGT1A9

Region	Promoter		Exon1			Frequency
Nucleotide change	-126_-118 T9>T10	-126_-118 T9>T11	422 C>G	726 T>G	766 G>A	
Amino acid change			S141C	Y242X	D256N	Frequency
Marker allele	*22	*T11	*141C	*4	*5	

Haplotype							Frequency
	*1						0.347
	*22						0.644
	*141C						0.000
	*4						0.000
	*5						0.006
	*T11						0.003

Haplotypes of *UGT1A* gene segments (*UGT1A1, 1A7, 1A9, 1A10*, and Block C) in 177 Japanese cancer patients. The tagging variations and haplotypes are shown. Variant alleles are indicated in grey. Definition of Block C haplotypes in our previous paper ([14]) (corresponding to Block 2) were slightly modified.

Statistical analysis

Statistical analysis on the differences in the AUC ratios (SN-38G/SN-38) among *UGT1A* genotypes was performed using the Kruskal–Wallis test, followed by nonparametric Dunnett's multiple comparison test, or with Wilcoxon test. Analysis of a gene–dose effect of each haplotype was performed using the Jonckheere–Terpestra test in the SAS system, version 5.0 (SAS Institute, Cary, North Carolina, USA). Relationship of *UGT1A* genetic polymorphisms to the toxicities of irinotecan was assessed by the χ^2 test via the use of using Prism version 4.0 (GraphPad Prism Software, San Diego, California, USA). The *P*-value of 0.05 (two-tailed) was set as a significant level, and the multiplicity adjustment was conducted for pharmacokinetics data with the false discovery rate [30].

To identify factors associated with the log-transformed AUC ratio of SN-38G/SN-38, multiple regression analysis was performed using age, sex, body surface area, dosage of irinotecan, history of smoking or drinking, performance status, coadministered drugs, serum biochemistry parameters at baseline, and *1A9-1A7-1A1* and Block C haplotypes (five or more chromosome numbers) or '*1A1*6* or *28*. For multiple regression analysis of neutropenia, variables included the absolute neutrophil count at baseline and the dosing interval, in addition to

the other patient background factors described above. The multivariate analyses were performed by using JMP version 6.0.0 software (SAS Institute). The variables in the final models for both AUC ratio and neutropenia were chosen by forward and backward stepwise procedures at significance levels of 0.25 and 0.05, respectively.

Results

Patients and UGT1A haplotypes

Patient demographics and information on the treatment are summarized in Table 1. In addition to UGT1A1, UGT1A7, 1A9, and 1A10 were also reported to glucuronidate SN-38 [15–17]. In our previous study, haplotype analysis covering the *1A9* to *1A1* (5'–3') gene segments was conducted, and the combinatorial diplotypes (*1A9-1A7-1A1*) of the patients were determined. It must be noted that close linkages between *1A9*22* and *1A7*1*, between *1A7*2* and *1A1*60*, and between *1A7*3* and *1A1*6* or *1A1*28* were observed as described previously [28]. To clarify the linkages between these segmental haplotypes (*1A9*, *1A7*, and *1A1*), we grouped the combinatorial (*1A9-1A7-1A1*) haplotypes into four categories (A–D) based on the *1A1* haplotypes (*1*, *6*, *60*, and *28*). Each group was further divided into the subgroups based on the previously defined Block 9/6 (including *1A9*, *1A7*, and *1A6*) haplotypes (Table 2). The frequency of Group B haplotypes (*B1-B4*) harboring *1A1*6* was 0.167 and higher than that of Group D haplotypes (*D1-D6*) with *28* (0.138) in this population.

Association of 1A9-1A7-1A1 diplotypes to SN-38G formation

When relationship between the *UGT1A* diplotypes (*1A9-1A7-1A1*) and the SN-38G/SN-38 AUC ratio was analyzed

in the 176 cancer patients the AUC ratio for the diplotypes of *B2/B2*, *D2/A1*, and *D1/B2* was statistically significantly lower than the *A1/A1* diplotype (Fig. 2). These diplotypes harbored *1A1*6*, *28* or both. Significant gene–dose effects of *B2* (among *A1/A1*, *B2/A1*, and *B2/B2*) and *C3* (among *A1/A1*, *C3/A1*, and *C3/C3*) were also observed (Fig. 2). As no significant differences in AUC ratios were observed between *D1/A1* and *D2/A1*, *D1/C3* and *D2/C3*, and *D1/B2* and *D2/B2*, the haplotype combination *1A9*1-1A7*3* or *1A9*22-1A7*1* was not influential on the AUC ratio.

As the effect of diplotypes harboring *UGT1A1* polymorphism was prominent, we grouped the whole gene (*1A9-1A7-1A1*) diplotypes according to the *1A1* diplotypes (the upper part of Fig. 2). Patients with *6* or *28* (except for *28/*28) haplotypes had significantly lower AUC ratios than the wild-type (*1/*1), and significant gene–dose effects were observed for *28* (among *1/*1, *28/*1, and *28/*28) and *6* (among *1/*1, *6/*1 and *6/*6). A significant additive effect of *6* and *28* on the decreased AUC ratio was also observed when the values for *28/*1 were compared with those for *28/*6 (Fig. 2 and Table 3).

Regarding other polymorphisms, a statistically nonsignificant tendency to decrease the AUC ratio was observed for *60

Table 1 Characteristics of Japanese cancer patients in this study

		No. of participants	
Age			
Mean/range	60.5/26–78	177	
Sex			
Male/female		135/42	
Performance status	0/1/2	84/89/4	
Combination therapy and tumor type			
(initial dose of irinotecan; mg/m²)			
Irinotecan monotherapy	Lung (100)	21	
	Colon (150)	28	
	Others (100)	7	
With platinum-containing	Lung (60)	58[b]	48 [60][c]
drug[a]	Stomach (70)	9	9 [80][c]
	Others (60)	5	5 [80][c]
With 5-fluorouracil	Colon (100 or 150)	34	
(including tegafur)	Others (90 or 100)	2	
With mitomycin-C	Stomach (150)	10	
	Colon (150)	1	
With amrubicin	Lung (60)	2	
Previous treatment			
Surgery	Yes/no	85/92	
Chemotherapy	Yes/no	97/80	
Radiotherapy	Yes/no	26/151	
Smoking history	Yes/no	29/148	

[a]Cisplatin, cisplatin plus etoposide or carboplatla.
[b]Two and eight patients received cisplatin and etoposide and carboplatin, respectively.
[c]Number of cisplatin-administered patients [initial dose of cinlatin (mg/m²) is shown in brackets].

Table 2 Combinatorial haplotypes covering UGT1A9, UGT1A7, and UGT1A1

Haplotype	Block haplotype[a]			Combination of segmental haplotypes	Cancer patients	
	Block 9/6	Block 4	Block 3/1	1A9-1A7-1A1	N[b]	Frequency
A1[c]	*I	*1	*I	*22-*1-*1	189	0.534
	*I	*3	*I			
A3	*III	*1	*I	*1-*2-*1	2	0.006
A2	*II	*1	*I	*1-*3-*1	1	0.003
A4	*IV	*1	*I	*22-*3-*1	1	0.003
A5				*T11-*1-*1	1	0.003
B2[c]	*II	*1	*III			
	*II	*1	*VI	*1-*3-*6	47	0.133
	*II	*4	*VI			
B4	*IV	*1	*III	*22-*3-*6	6	0.017
B1	*I	*1	*III	*22-*1-*6	5	0.014
	*I	*1	*VI			
B3	*III	*1	*III	*1-*2-*6	1	0.003
C3[c]	*III	*3	*IV			
	*III	*1	*IV			
	*III	*3	*V	*1-*2-*60	44	0.124
	*III	*1	*V			
C1	*I	*3	*IV	*22-*1-*60	5	0.014
	*I	*1	*IV			
C2	*II	*3	*IV	*1-*3-*60	2	0.006
C7	*VII	*3	*V	*22-*2-*60	1	0.003
D1	*I	*1	*IIa	*22-*1-*28	23	0.065
	*I	*1	*IIc			
D2	*II	*1	*IIa			
	*II	*3	*IIa	*1-*3-*28	22	0.062
	*II	*1	*IIc			
D6	*VI	*1	*IIb	*1-*2-*28	4	0.011
				Total	354	1.000

[a]Block haplotypes described in Ref. [28] are shown for reference. 1A9 and 1A7 are included in block 9/6 and 1A1 is included in block 3/1.
[b]Number of chromosomes.
[c]Major combinatrial haplotypes.

Fig. 2
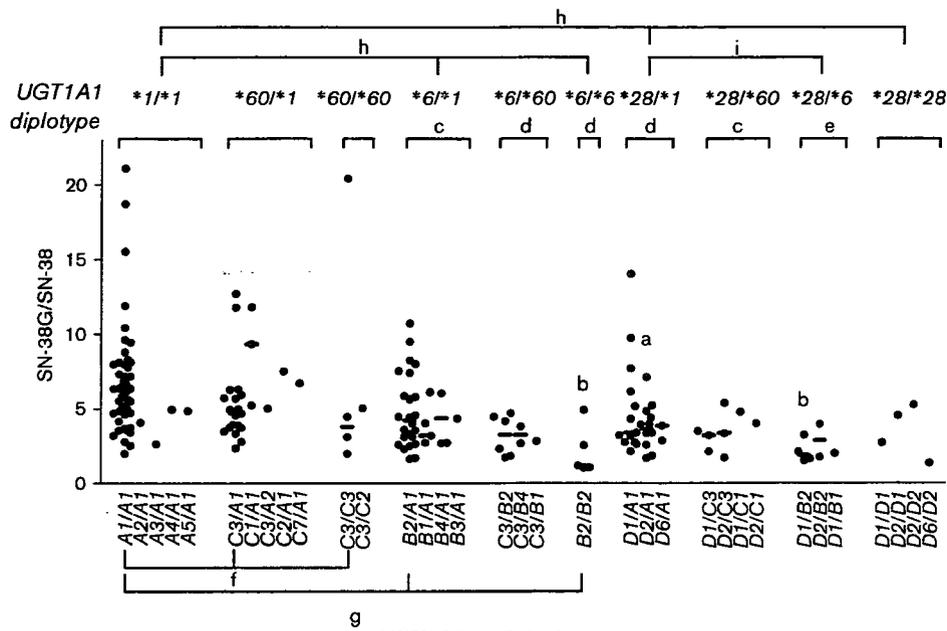
The association of *UGT1A* diplotypes with the reduced area under concentration curve (AUC) ratio (SN-38G/SN-38) in 176 Japanese cancer patients who received irinotecan. The whole gene (*1A9-1A7-1A1*) diplotypes are shown below the abscissa and the *UGT1A1* diplotypes are indicated in the upper part of the figure. Each point represents a patient value, and the median is indicated by a bar. Significant reductions in the AUC ratio were detected in the *B2/B2*, *D2/A1*, and *D1/B2* compared with *A1/A1* for the whole gene diplotypes [Kruskal–Wallis test (*P*=0.0009) followed by Dunnett's multiple comparison test]. As for the *1A1* diplotypes, significant reductions were detected in the *6/*1, *6/*60, *6/*6, *28/*1, *28/*60, and *28/*6 compared with the *1/*1 group [Kruskal–Wallis test (*P*<0.0001) followed by Dunnett's multiple comparison test]. Gene–dose effects on the reduced AUC ratio were significant for *6 and *28 (Jonckheere–Terpestra test). A significant additive effect of *6 on the reduced AUC ratio by *28 was detected by comparing *28/*1 and *28/*6. [a]*P*<0.05 and [b]*P*<0.01 against *A1/A1* group (Dunnett's multiple comparison test); [c]*P*<0.05, [d]*P*<0.01, and [e]*P*&<0.001 against the *1/*1 group (Dunnett's multiple comparison test); [f]*P*<0.05, [g]*P*<0.001, and [h]*P*<0.0001 (Jonckheere–Terpestra test for gene–dose effect); [i]*P*<0.01 (Wilcoxon test).

(*P* = 0.1134). No significant effects on the AUC ratio were observed for Block C (exon 2–5) haplotypes or rare variations including *1A10* (*2T*, *2*, or *3*) and *1A9* (*5*, *T11*).

Multiple regression analysis of the area under concentration curve ratio

We further assessed the impact of *UGT1A* genetic factors on the AUC ratio by multiple regression analysis. First, we used the *1A9-1A7-1A1* and Block C haplotypes as genetic factors. The AUC ratio was significantly associated with the haplotypes *B2*, *D1*, and *D2* and serum biochemistry parameters indicating hepatic or renal function before treatment. The Groups B and D haplotypes harbor *1A1*6* and *28*, respectively. The dependency on specific *1A7* or *1A9* polymorphisms, however, was not obtained, considering the contributions of both *D1* and *D2*. As *1A1*6* and *28* are mutually exclusive and their effects are comparable, we grouped *1A1*6* and *28* into the same category in the final multiple regression model (Table 4). The final model confirmed the significant contribution of this genetic marker (*6* or *28*) to the AUC ratio.

Effects of the genetic marker '*6 or *28' on pharmaco kinetic parameters

Then, a dose effect of the genetic marker '*6 or *28' on pharmacokinetic parameters was further analyzed

Table 3 AUC ratio of SN-38 glucuronide to SN-38 for *UGT1A1* diplotypes

| Diplotype | Number of patients | AUC ratio | | *P*-value[a] (vs. *1/*1) |
		Median	Interquartile range	
*1/*1	55	6.13	4.72–7.79	
*1/*60	25	5.04	3.85–6.52	0.9803
*60/*60	5	4.48	2.57–12.74	0.8141
*6/*1	32	4.03	2.74–5.97	0.0126
*6/*60	9	2.84	2.09–4.33	0.0021
*6/*6	5	1.19	1.06–3.74	0.0012
*28/*1	26	3.65	2.76–5.21	0.0040
*28/*60	8	3.44	2.68–4.40	0.0261
*28/*6	7	2.03	1.65–3.26	<0.0001
*28/*28	4	3.65	2.05–4.92	0.2322

AUC, area under concentration curve.
[a]Dunnett's multiple comparison test.

(Fig. 3). Patients with one haplotype harboring either *6 or *28 (*6/*1, *6/*60, *28/*1, and *28/*60) had lower SN-38G/SN-38 AUC ratios (median, 3.62; interquartile range, 2.74–5.18) than patients without *6 or *28 (*1/*1, *60/*1, and *60/*60) (5.55, 4.13–7.26), and patients with two haplotypes harboring *6 or *28 (*6/*6, *28/*28, and *28/*6) had the lowest AUC ratio (2.07, 1.45–3.62) (*P* < 0.0001, Fig. 3a). Similarly, the number of the *6 or *28-containing haplotypes affected the AUC ratios of SN-38 to irinotecan (Fig. 3b). When the correlations

between irinotecan dosage and the AUC of SN-38 were tested, different correlations were obtained according to the number of the haplotypes (Fig. 3c). The slope of regression line for one and two haplotypes harboring *6 or *28 was 1.4-fold and 2.4-fold greater, respectively, than that for the diplotype without *6 or *28.

Associations of UGT1A1 genetic polymorphisms with toxicities

Association between genetic polymorphisms and toxicities was investigated in patients receiving irinotecan as a single agent. One patient was referred to another hospital 3 days after the first administration of irinotecan without evaluating toxicities and was lost in terms of follow-up. Therefore, association between genetic polymorphisms and toxicities was investigated in 55 patients. Six (11%) and 14 (25%) patients experienced grade 3 or greater diarrhea and neutropenia, respectively. As for the 1A9-1A7-1A1 diplotypes, a higher incidence of grade 3 or greater neutropenia was observed in D1/B2 (1A1*28/*6) (100%, n = 3) than in A1/A1 (11.8%, n = 17) (P = 0.0088, Fisher's exact test), indicating clinical impact of the genetic marker 1A1*6 or *28. As for the dose effect of ‘*6 or *28’, incidences of grade 3 or 4 neutropenia were 14, 24, and 80% for 0, 1, and 2 haplotypes harboring these markers, respectively (Table 5). A significant association between ‘*6 or *28’and neutropenia was also observed for 62 patients who received irinotecan in combination with cisplatin (Table 5). No association, however, was observed between diarrhea and the marker ‘*6 or *28’.

Multivariate analysis for irinotecan toxicities

We further evaluated the effect of the genetic marker ‘*6 or *28’ on neutropenia in multivariate analysis, and confirmed a significant correlation of ‘*6 or *28’ with the nadir of absolute neutrophil counts (Table 6). Elevated alkaline phosphatase levels and the absolute neutrophil count at baseline were also significant.

Discussion

The association study with the 1A9-1A7-1A1 diplotypes revealed that the reduction in inactivation of SN-38, as well

Table 4 Multiple regression analysis toward the AUC ratio (SN-38G/SN-38)[a]

Variable	Coeffi-cient	F-value	P-value	R^2	Intercept	N
				0.410	0.8869	176
*6 or *28	-0.189	70.2	<0.0001			
Age	0.005	8.88	0.0033			
Serum albumin level[b]	-0.136	9.92	0.0019			
Serum GOT and ALP[c]	0.070	8.88	0.0033			
Serum creatinine[d]	0.210	7.23	0.0079			

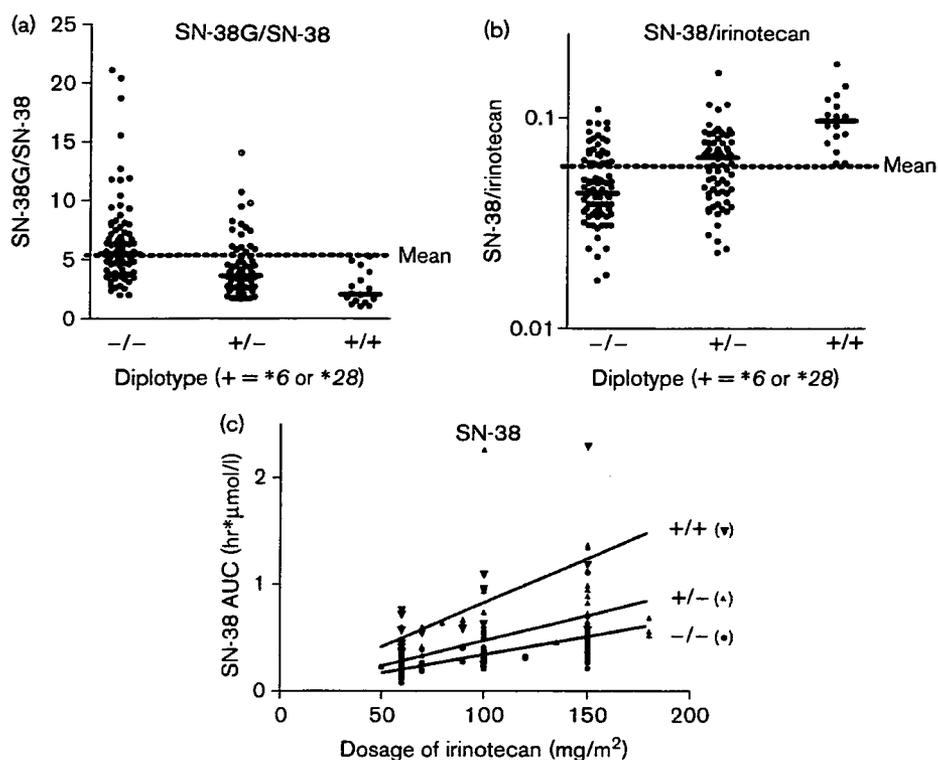ALP, alkaline phosphatase; AUC, area under concentration curve.
[a]The values after logarithmic conversion were used as an objective variable.
[b]The absolute value (g/dl) before irinotecan treatment.
[c]Grade 1 or greater scores in both serum GOT and ALP before irinotecan treatment.
[d]Grade 1 or greater scores in serum creatinine before irinotecan treatment.

as neutropenia, was dependent on the Groups B and D haplotypes which corresponded to the 1A1*6 and *28 segmental haplotypes. Also, multivariate analyses clearly showed clinical significance of the genetic marker ‘*6 or *28’ for both pharmacokinetics and toxicity of irinotecan in Japanese patients (Tables 3 and 6). UGT1A1*6 and *28 were mutually exclusive [14] and contributed to the reduction in glucuronidation of SN-38 to the same extent. Therefore, the activity of SN-38 glucuronidation in individuals depended on the number of the haplotypes harboring *6 or *28. Although the role of 1A1*28 for irinotecan toxicity has been focused on [8–12], this study strongly suggests that *6 should be tested in addition to *28 before starting chemotherapy with irinotecan in Japanese patients.

The clinical importance of *6 for neutropenia by irinotecan was also supported by a recent report in Korean patients who received irinotecan and cisplatin [31]. Although no patients with irinotecan as a single agent were homozygous for *6 in our study, clinical significance of the double heterozygote, *6/*28, was clearly demonstrated. Among patients treated with irinotecan in combination chemotherapy, the majority of patients received platinum agents in our study. A significant association of ‘*6 or *28’ with a higher incidence of grade 3 or 4 neutropenia was also observed in patients who received irinotecan and cisplatin (Table 5). These findings further support the necessity of testing ‘*6 or *28’ before irinotecan is given to patients.

As possible enhancement of toxicities by the *27 allele was suggested [8], we evaluated the effect of the *28c haplotype, which had an additional single-nucleotide polymorphism [*27; 686C > A(P229Q)] to the *28 allele (-40_-39insTA). In our cohort of patients, there were three *28c heterozygotes (*28c/*1) and one double heterozygote (*28b/*28c). The values of the AUC ratio were within the range of variations of the *28 group, and no additional impact of *28c was observed in relation to toxicities.

Although the decreasing trend of the AUC ratio for 1A1*60 (and combinatorial haplotype C3) was observed (Fig. 2), the contribution of 1A1*60 to toxicities was not clearly demonstrated in this study as reported in the Japanese retrospective study [32].

In addition to UGT1A1, recent studies have suggested possible contributions of UGT1A7, 1A9, and 1A10 to SN-38G formation [15–17]. An in-vitro study demonstrated that 1A7*3 [387T > G(N129K), 391C > A(R131K), 622T > C(W208R)] had reduced activity in terms of SN-38G formation [16]. Results of clinical studies, however, on the association between 1A7 polymorphisms and irinotecan toxicity/efficacy are inconsistent, whereas different populations with different combination therapies were used [19,20]. Furthermore, it was reported that the UGT1A7 polymorphisms (*2 and *3), which were linked to 1A9*1, were associated with a lowered incidence

Fig. 3

Effects of the genetic marker of *UGT1A1* '*6 or *28' on the area under concentration curve (AUC) ratios of SN-38G/SN-38 (a) and SN-38/irinotecan (b), and SN-38 by irinotecan dosage (c) in 176 Japanese cancer patients after irinotecan treatment.

Table 5 Association of *UGT1A1*6* and *28* with irinotecan toxicities

Diplotype (+ =*6 or *28)	Number of patients	Diarrhea (grade 3)	Neutropenia (grade 3 or 4)
Irinotecan monotherapy			
-/-	21	3 (14.3%)[a]	3 (14.3%)
+/-	29	2 (6.90%)	7 (24.1%)
+/+	5	1 (20.0%)	4 (80.0%)
P-value[b]		0.8500	**0.0117**
P-value[c]		0.3889	**0.0124**
With cisplatin			
-/-	35	1 (2.9%)	20 (57.1%)
+/-	20	2 (10.0%)	14 (70.0%)
+/+	7	1 (14.3%)	7 (100%)
P-value[b]		0.1747	**0.0315**
P-value[c]		0.3886	0.0863

[a]Percentage of the patient number in each diplotype is indicated in parentheses.
[b]Chi-squared test for trend.
[c]Fisher's exact test, (-/- and +/-) vs. +/+.

Table 6 Multiple regression analysis of the nadir of absolute neutrophil counts in the patients with irinotecan monotherapy

Variable	Coefficient	F-value	P-value	R^2	Intercept	N
				0.3942	643	53
Serum ALP[a]	-349.9	12.2	0.0010			
Neutrophil count before irinotecan treatment	0.2466	13.5	0.0006			
*6 or *28	-369.1	6.40	0.0146			

[a]Grade 1 or greater scores of serum ALP before irinotecan treatment.

of diarrhea in the irinotecan/capecitabine regimen, in which diarrhea was a major toxicity [20]. A highly frequent allele *1A9*22* with an insertion of T into the nine T repeats in the promoter region (-126_-118T$_9$ > T$_{10}$) was shown to have an enhanced promoter activity in an in-vitro reporter assay [21], whereas 1A9 protein expression levels did not change in the clinical samples [22]. Rare variations, *1A9*5* [766G > A(D256N)] and *UGT1A10*3* [605C > T(T202I)], were shown to cause reduced activity *in vitro*, but their clinical importance is still unknown [23,24]. Moreover, close linkages among *1A9*, *1A7*, and *1A1*

polymorphisms were found in Caucasians and Asians in an ethnic-specific manner [20,25–28].

Our study also revealed close linkages between *1A9*22* and *1A7*1*, *1A7*3* and *1A1*6* or *28* [28]. This fact makes it difficult to draw firm conclusions about the effects of *1A7*3* and *1A9*22* themselves. It is, however, reasonable to conclude that the degree of neutropenia depends on the activity of UGT1A1, because UGT1A1 is a major UGT1A enzyme in the liver and plays a primary role for regulating plasma concentrations of SN-38.

Taken together, for practical application to individualized irinotecan therapy, genotyping of *UGT1A1*6* and *28* would be beneficial and necessary in Japanese cancer patients to avoid severe adverse reactions. The frequency

of homozygotes for '*6 or *28' (namely, *6/*6, *6/*28, and *28/*28) is approximately 10%, which is comparable to the frequency of *28 homozygotes in Caucasian populations. In our study, it may be difficult to establish definite guidelines for dose reductions of irinotecan for patients homozygous for '*6 or *28'. Considering, however, 2.4-fold steep relationship between the dose of irinotecan and the AUC of SN-38 for patients homozygous for '*6 or *28' compared with patients without '*6 or *28' (Fig. 3c), the dose for patients homozygous for '*6 or *28' should be reduced to a half of the dosage recommended for other patients. Prospective studies are necessary to confirm the validity of the recommendation for dose reduction in Japanese cancer patients homozygous for '*6 or *28'.

Acknowledgements

References

1   Garcia-Carbonero R, Supko JG. Current perspectives on the clinical experience, pharmacology, and continued development of the camptothecins. Clin Cancer Res 2002; 8:641–661.

2   Slatter JG, Su P, Sams JP, Schaaf LJ, Wienkers LC. Bioactivation of the anticancer agent CPT-11 to SN-38 by human hepatic microsomal carboxylesterases and the in vitro assessment of potential drug interactions. Drug Metab Dispos 1997; 25:1157–1164.

3   Iyer L, King CD, Whitington PF, Green MD, Roy SK, Tephly TR, et al. Genetic predisposition to the metabolism of irinotecan (CPT-11). Role of uridine diphosphate glucuronosyltransferase isoform 1A1 in the glucuronidation of its active metabolite (SN-38) in human liver microsomes. J Clin Invest 1998; 101:847–854.

4   De Forni M, Bugat R, Chabot GG, Culine S, Extra JM, Gouyette A, et al. Phase I and pharmacokinetic study of the camptothecin derivative irinotecan, administered on a weekly schedule in cancer patients. Cancer Res 1994; 54:4347–4354.

5   Gupta E, Lestingi TM, Mick R, Ramirez J, Vokes EE, Ratain MJ. Metabolic fate of irinotecan in humans: correlation of glucuronidation with diarrhea. Cancer Res 1994; 54:3723–3725.

6   Hanioka N, Ozawa S, Jinno H, Ando M, Saito Y, Sawada J. Human liver UDP-glucuronosyltransferase isoforms involved in the glucuronidation of 7-ethyl-10-hydroxycamptothecin. Xenobiotica 2001; 31:687–699.

7   Fisher MB, VandenBranden M, Findlay K, Burchell B, Thummel KE, Hall SD, et al. Tissue distribution and interindividual variation in human UDP-glucuronosyltransferase activity: relationship between UGT1A1 promoter genotype and variability in a liver bank. Pharmacogenetics 2000; 10:727–739.

8   Ando Y, Saka H, Ando M, Sawa T, Muro K, Ueoka H, et al. Polymorphisms of UDP-glucuronosyltransferase gene and irinotecan toxicity: a pharmacogenetic analysis. Cancer Res 2000; 60:6921–6926.

9   Iyer L, Das S, Janisch L, Wen M, Ramirez J, Karrison T, et al. UGT1A1*28 polymorphism as a determinant of irinotecan disposition and toxicity. Pharmacogenomics J 2002; 2:43–47.

10 Innocenti F, Undevia SD, Iyer L, Chen PX, Das S, Kocherginsky M, et al. Genetic variants in the UDP-glucuronosyltransferase 1A1 gene predict the risk of severe neutropenia of irinotecan. J Clin Oncol 2004; 22:1382–1388.

11 Marcuello E, Altes A, Menoyo A, del Rio E, Gomez-Pardo M, Baiget M. UGT1A1 gene variations and irinotecan treatment in patients with metastatic colorectal cancer. Br J Cancer 2004; 91:678–682.

12 Rouits E, Boisdron-Celle M, Dumont A, Guerin O, Morel A, Gamelin E. Relevance of different UGT1A1 polymorphisms in irinotecan-induced

13 Kaniwa N, Kurose K, Jinno H, Tanaka-Kagawa T, Saito Y, Saeki M, et al. Racial variability in haplotype frequencies of UGT1A1 and glucuronidation activity of a novel single nucleotide polymorphism 686C>T (P229L) found in an African-American. Drug Metab Dispos 2005; 33:458–465.

14 Sai K, Saeki M, Saito Y, Ozawa S, Katori N, Jinno H, et al. UGT1A1 haplotypes associated with reduced glucuronidation and increased serum bilirubin in irinotecan-administered Japanese patients with cancer. Clin Pharmacol Ther 2004; 75:501–515.

15 Ciotti M, Basu N, Brangi M, Owens IS. Glucuronidation of 7-ethyl-10-hydroxycamptothecin (SN-38) by the human UDP-glucuronosyltransferases encoded at the UGT1 locus. Biochem Biophys Res Commun 1999; 260:199–202.

16 Gagne JF, Montminy V, Belanger P, Journault K, Gaucher G, Guillemette C. Common human UGT1A polymorphisms and the altered metabolism of irinotecan active metabolite 7-ethyl-10-hydroxycamptothecin (SN-38). Mol Pharmacol 2002; 62:608–617.

17 Oguri T, Takahashi T, Miyazaki M, Isobe T, Kohno N, Mackenzie PI. UGT1A10 is responsible for SN-38 glucuronidation and its expression in human lung cancers. Anticancer Res 2004; 24:2893–2896.

18 Basu NK, Ciotti M, Hwang MS, Kole L, Mitra PS, Cho JW, et al. Differential and special properties of the major human UGT1-encoded gastrointestinal UDP-glucuronosyltransferases enhance potential to control chemical uptake. J Biol Chem 2004; 279:1429–1441.

19 Ando M, Ando Y, Sekido Y, Ando M, Shimokata K, Hasegawa Y. Genetic polymorphisms of the UDP-glucuronosyltransferase 1A7 gene and irinotecan toxicity in Japanese cancer patients. Jpn J Cancer Res 2002; 93:591–597.

20 Carlini LE, Meropol NJ, Bever J, Andria ML, Hill T, Gold P, et al. UGT1A7 and UGT1A9 polymorphisms predict response and toxicity in colorectal cancer patients treated with capecitabine/irinotecan. Clin Cancer Res 2005; 11:1226–1236.

21 Yamanaka H, Nakajima M, Katoh M, Hara Y, Tachibana O, Yamashita J, et al. A novel polymorphism in the promoter region of human UGT1A9 gene (UGT1A9*22) and its effects on the transcriptional activity. Pharmacogenetics 2004; 14:329–332.

22 Girard H, Court MH, Bernard O, Fortier LS, Villeneuve L, Hao Q, et al. Identification of common polymorphisms in the promoter of the UGT1A9 gene: evidence that UGT1A9 protein and activity levels are strongly genetically controlled in the liver. Pharmacogenetics 2004; 14:501–515.

23 Jinno H, Saeki M, Saito Y, Tanaka-Kagawa T, Hanioka N, Sai K, et al. Functional characterization of human UDP-glucuronosyltransferase 1A9 variant, D256N, found in Japanese cancer patients. J Pharmacol Exp Ther 2003; 306:688–693.

24 Jinno H, Saeki M, Tanaka-Kagawa T, Hanioka N, Saito Y, Ozawa S, et al. Functional characterization of wild-type and variant (T202I and M59I) human UDP-glucuronosyltransferase 1A10. Drug Metab Dispos 2003; 31:528–532.

25 Kohle C, Mohrle B, Munzel PA, Schwab M, Wernet D, Badary OA, et al. Frequent co-occurrence of the TATA box mutation associated with Gilbert's syndrome (UGT1A1*28) with other polymorphisms of the UDP-glucuronosyltransferase-1 locus (UGT1A6*2 and UGT1A7*3) in Caucasians and Egyptians. Biochem Pharmacol 2003; 65:1521–1527.

26 Huang MJ, Yang SS, Lin MS, Huang CS. Polymorphisms of uridine-diphosphoglucuronosyltransferase 1A7 gene in Taiwan Chinese. World J Gastroenterol 2005; 11:797–802.

27 Innocenti F, Liu W, Chen P, Dedai AA, Das S, Ratain MJ. Haplotypes of variants in the UDP-glucuronosyltransferase 1A9 and 1A1 genes. Pharmacogenet Genomics 2005; 15:295–301.

28 Saeki M, Saito Y, Jinno H, Sai K, Ozawa S, Kurose K, et al. Haplotype structures of the UGT1A gene complex in a Japanese population. Pharmacogenomics J 2006; 6:63–75.

29 Sai K, Kaniwa N, Ozawa S, Sawada J. An analytical method for irinotecan (CPT-11) and its metabolites using a high-performance liquid chromatography: parallel detection with fluorescence and mass spectrometry. Biomed Chromatogr 2002; 16:209–218.

30 Benjamini Y, Hochberg Y. Controlling the false discovery rate: a practical and powerful approach to multiple testing. J Roy Stat Soc B 1995; 57:289–300.

31 Han JY, Lim HS, Shin ES, Yoo YK, Park YH, Lee JE, et al. Comprehensive analysis of UGT1A polymorphisms predictive for pharmacokinetics and treatment outcome in patients with non-small-cell lung cancer treated with irinotecan and cisplatin. J Clin Oncol 2006; 24:2237–2244.

32 Kitagawa C, Ando M, Ando Y, Sekido Y, Wakai K, Imaizumi K, et al. Genetic polymorphism in the phenobarbital-responsive enhancer module of the UDP-glucuronosyltransferase 1A1 gene and irinotecan toxicity. Pharmacogenet Genomics 2005; 15:35–41.

ORIGINAL ARTICLE

Analysis of *ENG* and *ACVRL1* genes in 137 HHT Italian families identifies 76 different mutations (24 novel). Comparison with other European studies

Carla Olivieri · Fabio Pagella · Lucia Semino · Luca Lanzarini ·
Cristina Valacca · Andrea Pilotto · Sabrina Corno · Susi Scappaticci ·
Guido Manfredi · Elisabetta Buscarini · Cesare Danesino

Abstract Hereditary hemorrhagic telangiectasia (HHT) is an autosomal dominant disorder causing vascular dysplasias. About 70–80% of HHT patients carries mutations in *ENG* or *ACVRL1* genes, which code for a TGFβ receptor type III and I respectively. Molecular data on a large cohort of Italian HHT patients are presented, discussing the significance of missense and splice site mutations. Mutation analysis in *ENG* and *ACVRL1* genes was performed using single strand conformation polymorphisms (SSCP), denaturing high performance liquid chromatography (DHPLC) and subsequent direct sequencing. Overall, 101 mutations were found, with *ACVRL1* involved in 71% of cases. The highest number of mutations (28/101 subjects, 14/76 different mutations referring to both genes) was in *ACVRL1*,

exon 3. Mutation analysis was then extended to a total of 356 family members, and 162 proven to carry the mutation. New polymorphisms were identified in both genes, and evidence that ENG P131L change is not a disease-causing mutation was also provided. An in silico analysis was performed in order to characterize splice-site mutations. These results were compared to other European national studies and data from Italy, France and Spain were consistent for an higher incidence of *ACVRL1* mutations.

Keywords Hereditary hemorrhagic telangiectasia ·
HHT · *ACVRL1* mutation · *ENG* mutation

C. Olivieri · C. Valacca · S. Scappaticci · C. Danesino (✉)
Biologia Generale e Genetica Medica, University of Pavia,
Via Forlanini, 14, 27100 Pavia, Italy
e-mail: cidi@unipv.it

F. Pagella · L. Semino · S. Corno
Clinica Otorinolaringoiatrica, Fondazione IRCCS Policlinico
"S. Matteo", Pavia, Italy

L. Lanzarini
Divisione di Cardiologia, Fondazione IRCCS Policlinico
"S. Matteo", Pavia, Italy

A. Pilotto
Centre for Inherited Cardiovascular Diseases, Fondazione
IRCCS Policlinico "S. Matteo", Pavia, Italy

G. Manfredi · E. Buscarini
U. O. Gastroenterologia, Ospedale Maggiore di Crema,
Crema, Italy

C. Danesino
Servizio di Consulenza Genetica, Fondazione IRCCS
Policlinico "S. Matteo", Pavia, Italy

Introduction

Hereditary hemorrhagic telangiectasia (HHT; Mutation Database: http://137.195.14.43/cgi-bin/WebObjects/hht.woa/wa/default) is an autosomal dominant disorder causing vascular dysplasias such as mucocutaneous telangiectases and arterovenous malformations (AVMs). Telangiectases may lead to epistaxes and gastrointestinal bleeding, which may be severe enough to require transfusions. Epistaxes and telangiectases are the most frequent symptoms, present in more than 95% of the patients. AVMs are mostly observed in liver (60%), lungs (18–70%) and brain (6%), and may cause severe life-threatening complications (Lesca et al. 2007). The phenotype is highly variable, even among members of the same family, and the disease displays age-related penetrance, with increased manifestations developing over a lifetime. About 70–80% of HHT patients carry mutations in either of two genes—*ENG* (OMIM #131195) (HHT1: OMIM 187300) or *ACVRL1* (OMIM #601284) (HHT2: OMIM 600376)—which code for a TGFβ receptor type III and I respectively, although David

cancer patients with 5-fluorouracil-related side effects. Hum Mutat 22:498

Grem JL (1996) Fluoropyrimidines. In: Chabner BA, Longo DL (eds) Cancer chemotherapy and biotherapy, 2nd edn. Lippincott-Raven, Philadelphia, pp 149–197

Heggie GD, Sommadossi JP, Cross DS, Huster WJ, Diasio RB (1987) Clinical pharmacokinetics of 5-fluorouracil and its metabolites in plasma, urine, and bile. Cancer Res 47:2203–2206

Hormozian F, Schmitt JG, Sagulenko E, Schwab M, Savelyeva L (2007) *FRA1E* common fragile site breaks map within a 370 kilobase pair region and disrupt the dihydropyrimidine dehydrogenase gene (*DPYD*). Cancer Lett 246:82–91

Hsiao HH, Yang MY, Chang JG, Liu YC, Liu TC, Chang CS, Chen TP, Lin SF (2004) Dihydropyrimidine dehydrogenase pharmacogenetics in the Taiwanese population. Cancer Chemother Pharmacol 53:445–451

Johnson MR, Wang K, Diasio RB (2002) Profound dihydropyrimidine dehydrogenase deficiency resulting from a novel compound heterozygote genotype. Clin Cancer Res 8:768–774

Kitamura Y, Moriguchi M, Kaneko H, Morisaki H, Morisaki T, Toyama K, Kamatani N (2002) Determination of probability distribution of diplotype configuration (diplotype distribution) for each subject from genotypic data using the EM algorithm. Ann Hum Genet 66: 183–193

Kouwaki M, Hamajima N, Sumi S, Nonaka M, Sasaki M, Dobashi K, Kidouchi K, Togari H, Wada Y (1998) Identification of novel mutations in the dihydropyrimidine dehydrogenase gene in a Japanese patient with 5-fluorouracil toxicity. Clin Cancer Res 4:2999–3004

Lu Z, Zhang R, Diasio RB (1993) Dihydropyrimidine dehydrogenase activity in human peripheral blood mononuclear cells and liver: population characteristics, newly identified deficient patients, and clinical implication in 5-fluorouracil chemotherapy. Cancer Res 53:5433–5438

Lu Z, Zhang R, Carpenter JT, Diasio RB (1998) Decreased dihydropyrimidine dehydrogenase activity in a population of patients with breast cancer: implication for 5-fluorouracil-based chemotherapy. Clin Cancer Res 4:325–329

Martz E (2002) Protein explorer: easy yet powerful macromolecular visualization. Trends Biochem Sci 27:107–109

Mattison LK, Johnson MR, Diasio RB (2002) A comparative analysis of translated dihydropyrimidine dehydrogenase cDNA; conservation of functional domains and relevance to genetic polymorphisms. Pharmacogenetics 12:133–144

McLeod HL, Collie-Duguid ES, Vreken P, Johnson MR, Wei X, Sapone A, Diasio RB, Fernandez-Salguero P, van Kuilenberg AB, van Gennip AH, Gonzalez FJ (1998) Nomenclature for human DPYD alleles. Pharmacogenetics 8:455–459

Morel A, Boisdron-Celle M, Fey L, Soulie P, Craipeau MC, Traore S, Gamelin E (2006) Clinical relevance of different dihydropyrimidine dehydrogenase gene single nucleotide polymorphisms on 5-fluorouracil tolerance. Mol Cancer Ther 5:2895–2904

Naguib FN, el Kouni MH, Cha S (1985) Enzymes of uracil catabolism in normal and neoplastic human tissues. Cancer Res 45:5405–5412

Nishiyama T, Ogura K, Okuda H, Suda K, Kato A, Watabe T (2000) Mechanism-based inactivation of human dihydropyrimidine dehydrogenase by (E)-5-(2-bromovinyl)uracil in the presence of NADPH. Mol Pharmacol 57:899–905

Ogura K, Ohnuma T, Minamide Y, Mizuno A, Nishiyama T, Nagashima S, Kanamaru M, Hiratsuka A, Watabe T, Uematsu T (2005) Dihydropyrimidine dehydrogenase activity in 150 healthy Japanese volunteers and identification of novel mutations. Clin Cancer Res 11:5104–5111

Ridge SA, Sludden J, Brown O, Robertson L, Wei X, Sapone A, Fernandez-Salguero PM, Gonzalez FJ, Vreken P, van Kuilenburg AB, van Gennip AH, McLeod HL (1998a) Dihydropyrimidine dehydrogenase pharmacogenetics in Caucasian subjects. Br J Clin Pharmacol 46:151–156

Ridge SA, Sludden J, Wei X, Sapone A, Brown O, Hardy S, Canney P, Fernandez-Salguero P, Gonzalez FJ, Cassidy J, McLeod HL (1998b) Dihydropyrimidine dehydrogenase pharmacogenetics in patients with colorectal cancer. Br J Cancer 77:497–500

Seck K, Riemer S, Kates R, Ullrich T, Lutz V, Harbeck N, Schmitt M, Kiechle M, Diasio R, Gross E (2005) Analysis of the DPYD gene implicated in 5-fluorouracil catabolism in a cohort of Caucasian individuals. Clin Cancer Res 11:5886–5892

Shestopal SA, Johnson MR, Diasio RB (2000) Molecular cloning and characterization of the human dihydropyrimidine dehydrogenase promoter. Biochim Biophys Acta 1494:162–169

van Kuilenburg AB (2004) Dihydropyrimidine dehydrogenase and the efficacy and toxicity of 5-fluorouracil. Eur J Cancer 40:939–950

van Kuilenburg AB, Haasjes J, Richel DJ, Zoetekouw L, Van Lenthe H, De Abreu RA, Maring JG, Vreken P, van Gennip AH (2000) Clinical implications of dihydropyrimidine dehydrogenase (DPD) deficiency in patients with severe 5-fluorouracil-associated toxicity: identification of new mutations in the DPD gene. Clin Cancer Res 6:4705–4712

van Kuilenburg AB, Dobritzsch D, Meinsma R, Haasjes J, Waterham HR, Nowaczyk MJ, Maropoulos GD, Hein G, Kalhoff H, Kirk JM, Baaske H, Aukett A, Duley JA, Ward KP, Lindqvist Y, van Gennip AH (2002) Novel disease-causing mutations in the dihydropyrimidine dehydrogenase gene interpreted by analysis of the three-dimensional protein structure. Biochem J 364:157–163

Vreken P, Van Kuilenburg AB, Meinsma R, van Gennip AH (1997) Dihydropyrimidine dehydrogenase (DPD) deficiency: identification and expression of missense mutations C29R, R886H and R235W. Hum Genet 101:333–338

Wei X, Elizondo G, Sapone A, McLeod HL, Raunio H, Fernandez-Salguero P, Gonzalez FJ (1998) Characterization of the human dihydropyrimidine dehydrogenase gene. Genomics 51:391–400

Yamaguchi K, Arai Y, Kanda Y, Akagi K (2001) Germline mutation of dihydropyrimidine dehydrogenese gene among a Japanese population in relation to toxicity to 5-Fluorouracil. Jpn J Cancer Res 92:337–342

Zhang K, Qin Z, Chen T, Liu JS, Waterman MS, Sun F (2005) HapBlock: haplotype block partitioning and tag SNP selection software using a set of dynamic programming algorithms. Bioinformatics 21:131–134

Zhu AX, Puchalski TA, Stanton VP Jr, Ryan DP, Clark JW, Nesbitt S, Charlat O, Kelly P, Kreconus E, Chabner BA, Supko JG (2004) Dihydropyrimidine dehydrogenase and thymidylate synthase polymorphisms and their association with 5-fluorouracil/leucovorin chemotherapy in colorectal cancer. Clin Colorectal Cancer 3:225–234

Fig. 5 Stereo view of the variation sites in pig DPD (accession code of the Protein Data Bank: 1gth). Glu265 (a), Arg592 (b) and their adjacent residues are shown as *ball-and-stick* models with oxygens in *red*, nitrogens in *blue*, carbons in *gray* and sulfur in *yellow*. The adenosine moiety of the cofactor FAD is also shown in *pink* (a)
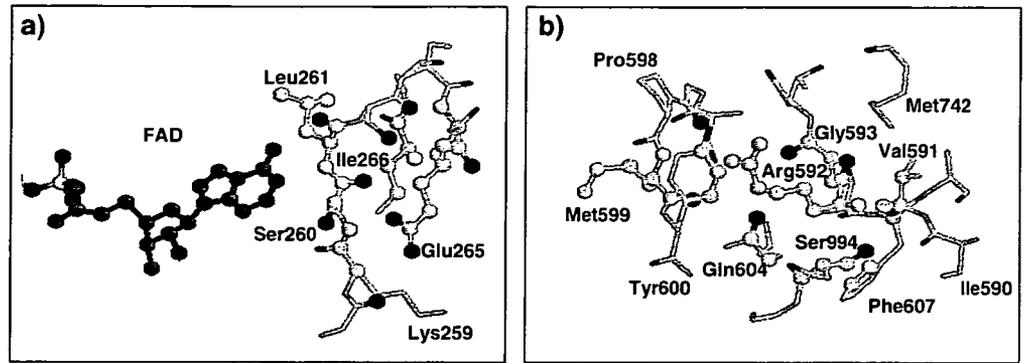
Japanese and Caucasians). HapMap data on 44 unrelated Japanese subjects showed that 476 variations are polymorphic, whereas 529 are monomorphic, and the average density of polymorphic markers is 1 SNP per 1,772 bp. In contrast, our study focused on exons and surrounding introns to detect variations, and only nine variations overlapped with the HapMap data. Therefore, we could not utilize the HapMap data to further identify common subtypes of [#]1 to be discriminated by many intronic HapMap SNPs in each block. However, most of the frequent SNPs are unlikely to be associated with substantially decreased DPD activity because DPD activity in the healthy Japanese population ($N = 150$) showed a unimodal Gaussian distribution (Ogura et al. 2005).

On the other hand, in 60 unrelated Caucasian subjects in the HapMap project, 617 are polymorphic, whereas 383 are monomorphic. LD profiles of these polymorphisms were compared between Caucasians and Japanese by using the program Marker (http://www.gmap.net/marker). Strong LD (ID'I > 0.75) clearly decays within introns 11, 12, 13, 14, 16, 18, and 20 in Japanese, whereas, similar decays are observed within introns 13, 14, 18, and 20, but are not obvious within introns 11, 12, and 16 in Caucasians (data not shown). Moreover, strong LD decays within intron 3 in Caucasians. Therefore, the LD blocks are considerably different between Japanese and Caucasians. Along with the marked differences in allele frequencies of several variations (Table 4), these results suggest that the haplotype structures in *DPYD* are quite different between the two populations.

In conclusion, we found 55 variations, including 38 novel ones, in *DPYD* from 341 Japanese subjects. Nine novel nonsynonymous SNPs were found, some of which were assumed to have impact on the structure and function of DPD. As for known variations, we obtained their accurate allele frequencies in a Japanese population of a large size and showed that variations with clinical relevance do not overlap between Caucasians and Japanese. In Japanese, 2303C>A (Thr768Lys) and 1003G>T (Val335Leu) might play important roles in 5-FU-related toxicity. Along with

differences in haplotype structures between Japanese and Caucasians, these findings suggest that ethnic-specific tagging SNPs should be considered on genotyping *DPYD*. Thus, the present information would be useful for pharmacogenetic studies for evaluating the efficacy and toxicity of 5-FU in Japanese and probably in East Asians.

References

Bakkeren JA, De Abreu RA, Sengers RC, Gabreels FJ, Maas JM, Renier WO (1984) Elevated urine, blood and cerebrospinal fluid levels of uracil and thymine in a child with dihydrothymine dehydrogenase deficiency. Clin Chim Acta 140:247–256

Barrett JC, Fry B, Maller J, Daly MJ (2005) Haploview: analysis and visualization of LD and haplotype maps. Bioinformatics 21:263–265

Cho HJ, Park YS, Kang WK, Kim JW, Lee SY (2007) Thymidylate synthase (TYMS) and dihydropyrimidine dehydrogenase (DPYD) polymorphisms in the Korean population for prediction of 5-fluorouracil-associated toxicity. Ther Drug Monit 29:190–196

Collie-Duguid ES, Etienne MC, Milano G, McLeod HL (2000) Known variant DPYD alleles do not explain DPD deficiency in cancer patients. Pharmacogenetics 10:217–223

Dobritzsch D, Schneider G, Schnackerz KD, Lindqvist Y (2001) Crystal structure of dihydropyrimidine dehydrogenase, a major determinant of the pharmacokinetics of the anti-cancer drug 5-fluorouracil. Embo J 20:650–660

Dobritzsch D, Ricagno S, Schneider G, Schnackerz KD, Lindqvist Y (2002) Crystal structure of the productive ternary complex of dihydropyrimidine dehydrogenase with NADPH and 5-iodouracil. Implications for mechanism of inhibition and electron transfer. J Biol Chem 277:13155–13166

Etienne MC, Lagrange JL, Dassonville O, Fleming R, Thyss A, Renee N, Schneider M, Demard F, Milano G (1994) Population study of dihydropyrimidine dehydrogenase in cancer patients. J Clin Oncol 12:2248–2253

Gross E, Ullrich T, Seck K, Mueller V, de Wit M, von Schilling C, Meindl A, Schmitt M, Kiechle M (2003) Detailed analysis of five mutations in dihydropyrimidine dehydrogenase detected in

Table 4 Allele frequencies of common *DPYD* SNPs in different populations

| Nucleotide change (amino acid change)	Allele or tagged haplotypes	Population	Allele frequency	Number of subjects	Reference
85T>C	*9	Caucasian	0.194	157	Seck et al. 2005
(Cys29Arg)	(Block 1 #9)	French Caucasian	0.185	487	Morel et al. 2006
		Japanese	0.037	107	Yamaguchi et al. 2001
		Japanese	0.029	341	This study
		Taiwanese	0.022	300	Hsiao et al. 2004
496A>G	Block 1 #166V	Caucasian	0.080	157	Seck et al. 2005
(Met166Val)		Japanese	0.022	341	This study
IVS10-15T>C	Block 1 #166Va, #9d	Caucasian	0.127	157	Seck et al. 2005
		Japanese	0.018	341	This study
1627A>G	*5	Caucasian	0.140	157	Seck et al. 2005
(Ile543Val)	(Block 2 #5)	Caucasian	0.275	60	Ridge et al. 1998a
		Finnish	0.072	90	Wei et al. 1998
		African-American	0.227	105	Wei et al. 1998
		Japanese	0.352	50	Wei et al. 1998
		Japanese	0.283	341	This study
		Taiwanese	0.210	131	Wei et al. 1998
		Taiwanese	0.283	300	Hsiao et al. 2004
1896T>C	Block 3 #1b	Caucasian	0.035	157	Seck et al. 2005
(Phe632Phe)		Japanese	0.098	107	Yamaguchi et al. 2001
		Japanese	0.139	341	This study
		Han Chinese	0.133	45	HapMap
IVS15 + 75A>G	Block 4 #1b	Caucasian	0.166	157	Seck et al. 2005
		Japanese	0.155	341	This study
IVS16-94G>T	Block 5 #1b	Caucasian	0.415	59	HapMap
		Yorba	ND	60	HapMap
		Japanese	0.455	44	HapMap
		Japanese	0.378	341	This study
		Han Chinese	0.333	45	HapMap
2194G>A	*6	Caucasian	0.022	157	Seck et al. 2005
(Val732Ile)	(Block 5 #6)	Caucasian	0.058	60	Ridge et al. 1998a
		Finnish	0.067	90	Wei et al. 1998
		African-American	0.019	105	Wei et al. 1998
		Japanese	0.044	50	Wei et al. 1998
		Japanese	0.015	341	This study
		Taiwanese	0.014	131	Wei et al. 1998
		Taiwanese	0.012	300	Hsiao et al. 2004
IVS18-39G>A	Block 6 #1b	Caucasian	0.105	157	Seck et al. 2005
		Caucasian	0.100	60	HapMap
		Yorba	0.017	60	HapMap
		Japanese	0.044	45	HapMap
		Japanese	0.032	341	This study
		Han Chinese	0.022	45	HapMap
IVS22-69G>A	Block 6 #1f	Caucasian	0.183	60	HapMap
		Yorba	0.400	60	HapMap
		Japanese	ND	45	HapMap
		Japanese	0.003	341	This study
		Han Chinese	ND	45	HapMap

ND not detected

substitution Cys29Arg on the protein surface was unlikely to alter DPD activity. However, conflicting results were reported regarding *9 (Vreken et al. 1997, van Kuilenburg et al. 2000), *6 (van Kuilenburg et al. 2000), and Met166Val (van Kuilenburg et al. 2000; Gross et al. 2003). To interpret these inconsistencies, haplotype analysis of *DPYD* might be helpful. Especially for *9 and Met166Val

in Japanese, functional involvement of –477T>G (block 1 #9c and #9e), –243G>A (block 1 #9d), IVS10-15T>C (block 1 #9d and #166Va) and many other HapMap SNPs linked to *9 and Met166Val (Table 3) needs clarification.

The HapMap project provides genotype data of more than 1,000 sites located mostly in the intronic regions of *DPYD* for four different populations (Nigerian, Chinese,

Fig. 4 The combinations of block haplotypes in Japanese. *Thick lines* represent combinations with frequencies over 10%, and *thin lines* represent combinations with frequencies of 1.0–9.9%
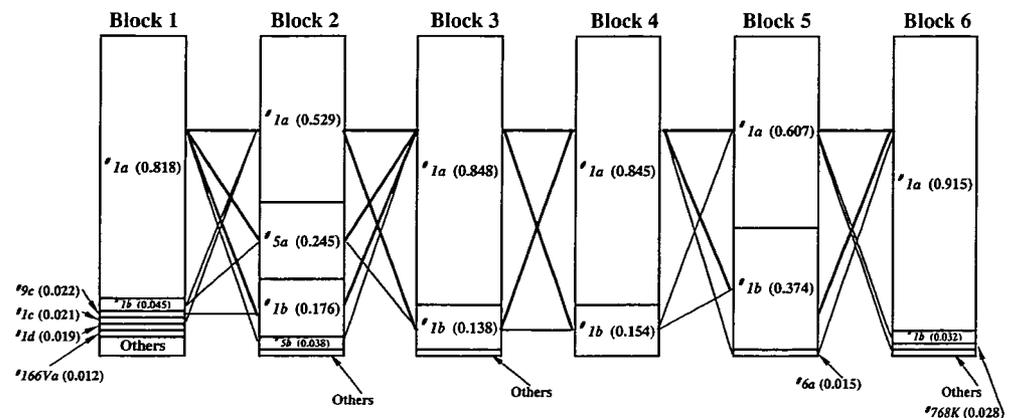
detected in the patient exhibiting severe mucositis during cyclophosphamide/methotrexate/5-FU chemotherapy (Gross et al. 2003). Furthermore, the adjacent Leu261 interacts via the main chain atoms with the N6, N1, and N3 atoms of adenine of FAD, and has an important role in the proper orientation of the adenine moiety in the FAD-binding pocket (Dobritzsch et al. 2001). Moreover, the carboxyl group (Glu265-Oε)might form hydrogen bonds to the main chain nitrogen of Ser260 next to Leu261. Thus, the change in polarity from negative to positive by the novel Glu265Lys substitution is likely to cause structural changes affecting proper binding of FAD.

Arg592 is located at one (IVβc) of the additional four-stranded antiparallel β sheets (IVβc-βf) inserted at the top of a typical $(\alpha/\beta)_8$ barrel fold in the FMN-binding domain IV (Dobritzsch et al. 2001). Arg592 is completely conserved among the above-mentioned six species (Mattison et al. 2002), suggesting its functional importance. Arg592 closely contacts Met599 (2.9 Å) and Gln604 (2.8 Å) in the same subunit and Ser994 (2.9 Å) in another subunit (Fig. 5B). The substitution of tryptophan for Arg592 is likely to weaken these interactions due to altered hydrophobicity and electrostatic changes. Arg592Trp was recently reported from a Korean population with an allele frequency of 0.004, although its functional significance remains to be confirmed(Cho et al. 2007).

As for known *DPYD* alleles, their distributions in several populations are becoming more evident by recent reports. For example, IVS14 + 1G>A (*2) (van Kuilenburg 2004), 295_298delTCAT (Phe100SerfsX15, *7) (Seck et al. 2005), 1679T>G (Ile560Ser, *13) (Collie-Duguid et al. 2000; Morel et al. 2006) 2846A>T (Asp949Val) (Seck et al. 2005; Morel et al. 2006), all of which are associated with decreased DPD activities, are detected in Caucasians with allele frequencies of 0.01–0.02, 0.003, 0.001 and 0.006–0.008, respectively. However, none of them were detected in our Japanese samples, while 1003G>T (Val335Leu, *11) and 2303C>A (Thr768Lys) have been found only in Japanese, indicating

that variations with clinical relevance do not overlap between Caucasians and Japanese.

2303C>A (Thr768Lys), which was originally found in a Japanese female volunteer with very low DPD activity (Ogura et al. 2005), is relatively frequent in Japanese (allele frequency = 0.0279). Functional characterization in vitro revealed that 768Lys caused thermal instability of the variant protein without changing its affinity for NADPH or kinetic parameters toward 5-FU. Therefore, they might cause 5-FU-related toxicities in Japanese.

1003G>T (Val335Leu, *11) was found in a Japanese family with decreased DPD activity by Kouwaki et al. (1998). By in vitro expression in *E. coli*, they demonstrated that the variant protein with Leu335 showed a significant loss of activity (about 17% of the wild-type protein). Dobritzsch et al. (2001) suggested from the 3D structure of pig DPD that Val335Leu, in spite of a conservative change, disturbs packing interactions in the hydrophobic core formed by IIIβ3 and IIIα3 within the Rossman-motif, thereby affecting NADPH binding. In our study, heterozygous 1003G>T (Val335Leu) was found from a patient administrated 5-FU (allele frequency = 0.0015), who also has seven other variations: IVS12–11G>A, 1896T>C (Phe632Phe), and IVS16–94G>T are heterozygous, and 1627A>G (Ile543Val), IVS13 + 39C>T, IVS14–123C>A, and IVS15 + 75A>G are homozygous, indicating that at least Val335Leu is linked to Ile543Val (*5).

On the other hand, Caucasians and Japanese share four variations: *5 (Ile543Val), *9 (Cys29Arg), Met166Val, and *6 (Val732Ile), although their allele frequencies were different, especially for *9 (Table 4). Because they have not necessarily correlated with phenotypic changes (e.g., differences in DPD enzyme activity, 5-FU pharmacokinetics and pharmacodynamics) (Collie-Duguid et al. 2000; Johnson et al. 2002; Zhu et al. 2004; Seck et al. 2005; Ridge et al. 1998a, 1998b; Hsiao et al. 2004), all of these variations are generally accepted as common polymorphisms that result in unaltered function. Consistent with this, van Kuilenburg et al. (2002) suggested that the

Table 3 Linkages of haplotype-tagging SNPs with HapMap SNPs for *DPYD*

Haplotype-tagging SNPs in *DPYD*	dbSNP ID (NCBI)	Block haplotype in this paper	HapMap SNPs with close linkages ($r^2 > 0.8$)[a]
85T>C (Cys29Arg)	rs1801265	Block 1 [#]9	rs10747488, rs7526108, rs4421623, rs4379706, rs4523551,rs11165921, rs9661794, rs6677116, rs6604093, rs17379561, rs10747491, rs10747492, rs12062845, rs7524038, rs10875112, rs4394693, rs10875113, rs4970722, rs9727548, rs10875118, rs9662719, rs12077442, rs4394694, rs9727976, rs4246515, rs6692580
496A>G (Met166Val)	rs2297595	Block 1 [#]166V	rs2786543, rs2811215, rs2811214, rs2786544, rs2248658, rs11165897, rs2786490, rs2811203, rs2811202, rs2811200, rs2811198, rs2786503, rs2811196, rs2786505, rs2811195, rs2811194, rs12073839, rs6663670, rs7512910, rs2151563, rs2786509, rs3790387, rs3790389
1627A>G (Ile543Val)	rs1801159	Block 2 [#]5	rs1415682, rs952501, rs2811187, rs2786778, rs2786774, rs2811183, rs17116806, rs2786780, rs1801159, rs2786771, rs2297780, rs2297779, rs12729863
1896T>C (Phe632Phe)	rs7556439	Block 3 [#]1b	rs12073650
IVS16-94G>T	rs7556439	Block 5 [#]1b	rs693680, rs827500, rs499009, rs7518848, rs553388, rs507170, rs628959, rs991544, rs526645, rs1609519
IVS18-39G>A	rs12137711	Block 6 [#]1b	rs12120068, rs12116905

[a] All SNPs are in the same block

Taken together, our data demonstrated considerable differences in the haplotype distributions in blocks 1, 3 and 6 between Japanese and Caucasians.

Discussion

This study provides Japanese data on the genetic variations of *DPYD*, a gene encoding a key enzyme catalyzing degradation of the well-known anticancer drug 5-FU. Nine novel (Ala10Glu, Tyr109Asn, Asn151Asp, Ile245Phe, Glu265Lys, Val515Ile, Phe524Leu, Ser556Arg, and Asn893Ser) and seven known nonsynonymous variations (Cys29Arg, Met166Val, Val335Leu, Ile543Val, Arg592Trp, Val732Ile, and Thr768Lys) were found in our Japanese population (Table 2 and Fig. 1). The association analysis between the genotypes and 5-FU pharmacodynamics is now on-going.

Uneven distributions of coding SNPs over 23 *DPYD* exons were pointed out in the previous review by van Kuilenburg (2004). The author indicated that 81% of all reported variations were confined to exons 2–14, representing 61% of the coding sequences, and typical hotspots of variation were localized in exons 2, 6, and 13. Our Japanese data also revealed that 17 out of 21 coding variations (81%) were localized in exons 1–14, and that more than three variations were detected in exons 5, 13, and 14 (Fig. 1). Recently, Hormozian et al. (2007) have reported that the common chromosomal fragile site on 1p21.2, *FRA1E*, spans 370 kb of genomic sequence between

introns 8 and 18 of *DPYD*, and that its core region with the highest fragility is located between introns 12 and 16. The instability at the core of *FRA1E* might be associated with the high mutational rates and recombinogenic nature from intron 12 to 14 of *DPYD* (Fig. 1).

To estimate potential functional consequences of the amino acid substitutions, we examined whether the positions of amino acid changes are located in highly conserved areas or potentially critical regions of the molecule (for example, substrate recognition sites or binding regions of prosthetic groups). We also considered the locations of the residues in a three-dimensional (3D) framework provided by the crystal structures of pig DPD, which have recently been determined in complexes with NADPH and substrate (5-FU) (Dobritzsch et al. 2001) or inhibitors (Dobritzsch et al. 2002). The amino acid sequences of pig and human DPD are 93% identical (Mattison et al. 2002), and the substituted residues and their neighboring residues are conserved between both enzymes. From these points of view, it is speculated that at least two substitutions (Glu265Lys and Arg592Trp) might impact the structure and function of DPD as discussed below.

Glu265 is located on the loop following to the third β sheet (IIβ3) in the FAD binding domain II (Dobritzsch et al. 2001). Glu265 is conserved among four mammalian species (human, mouse, rat, and pig), although it is replaced with aspartic acid in bovine and *Drosophila melanogaster* DPDs (Mattison et al. 2002). In the 3D structure of pig DPD (Fig. 5a), Glu265 is in close proximity to Lys259. The substitution, Lys259Glu, was